

Article highlights.

- Transcutaneous vaccination holds great promise because skin has numerous varied immunocompetent cells.
- A number of clinical studies have been conducted for transcutaneous vaccination using TCI devices, such as the patch system and jet injector.
- TCI devices using microneedles, particularly self-dissolving microneedles, are attractive from both safety and efficacy aspects.
- For more effective transcutaneous vaccination, the development of adjuvants using TLR ligands is in progress.
- The accumulation of information and preparation of guidelines are important for practical use of transcutaneous vaccination.

This box summarizes key points contained in the article.

and that is attracting great attention is the transcutaneous immunization (TCI) system [9,10].

In this article, we summarize the recently developed pharmaceutical and physical strategies and adjuvants for the enhancement of TCI.

2. Skin as a vaccination target

The skin is an organ that is constantly exposed to the risk of invasion by foreign substances. It is composed of three layers: the stratum corneum (SC), epidermis and dermis (Figure 1). SC operates as a 'physical barrier' to limit substance penetration. In addition, the skin acts as an 'immunological barrier' and contains various immunocompetent cells, such as Langerhans cells (LCs), keratinocytes, dermal dendritic cells (dDCs), macrophages, mast cells and T cells [11-15]. Keratinocytes account for ~ 90% of the total epidermal cell population and play an important role in innate immunity in the skin by producing a wide range of cytokines, chemokines and antimicrobial peptides in response to challenge. LCs in the epidermis and dDCs in the dermis have critical roles as potent antigen-presenting cells (APCs) against external antigens. In TCI, LCs and dDCs capture antigens/pathogens, migrate to the peripheral draining lymph nodes, process and present the antigen to the naïve T cells and initiate immune responses. Additionally, some researchers have reported that LCs and dDCs have the different functions as APCs; LCs induce humoral immune response and dDCs perform antigen cross-presentation by MHC class I [16], and TCI could induce immunoglobulin A (IgA) production in mucosal tissues [17]. This suggests that antigen delivery to the epidermis and dermis beneath SC promotes the induction of a strong and/or various immune responses, such as humoral, cellular and mucosal immunity. However, administration of the antigen solution onto the skin surface fails to result in penetration of SC and delivery of sufficient antigen into the skin [18-20]. Therefore, a number of studies are underway to improve various transcutaneous vaccination systems (Figure 2).

3. Transcutaneous vaccination techniques

As it is not easy for large proteins and viral particles to penetrate SC under normal conditions, the following two major strategies for TCI have been developed: i) promote antigen permeation of the skin barrier and ii) deliver the antigen into the skin by physical methods in order to overcome the skin barrier. Several devices have undergone clinical studies (Table 1).

3.1 Promoting antigen penetration through SC

Studies have been reported in which transcutaneous permeation of the antigen is increased, rendering it more readily available for uptake by APCs. In addition, the development of micro/nanometer drug delivery systems, such as liposomes and nanoparticles, as alternatives for transcutaneous vaccination is attracting attention.

3.1.1 Patch

The patch is one of the most commonly used systems for transcutaneous vaccination. Glenn *et al.* and McKenzie *et al.* reported that application of the vaccine patch (containing 50 µg *Escherichia coli* heat-labile toxin; LT) after removal of SC by tape stripping, increases the IgG titer to levels comparable to those obtained after active toxin infection and those induced by the oral cholera vaccine [21,22]. This vaccination system, known as the skin preparation system (SPS) was successful in Phase I and Phase II clinical studies against travelers' diarrhea (Table 1) [23,24]. Both preclinical and clinical investigations have shown that TCI results in mucosal immunity to LT, which may contribute to protection [22,24]. Moreover, influenza vaccination with LT using SPS showed improved immune responses in the elderly [25]. A cyanoacrylate skin surface stripping (CSSS) procedure has been developed for removing SC [26-28]. Transcutaneous influenza vaccination using CSSS promoted both CD4 and CD8 T-cell immune responses in humans (Table 1) [27,28]. In addition, cytotoxic T cells (CTLs) were induced by peptide immunization against melanoma using CSSS [26]. However, the development of a more easy-to-use and safer vaccination patch system is expected because SPS or CSSS require treatment to disrupt SC before patch application.

We have developed a hydrogel patch that was shown to induce effective immune responses against tetanus toxoid (TT) and diphtheria toxoid (DT) after application in the absence of any treatment (Figure 2A) [29-32]. The hydrogel patch was prepared with cross-linked HiPASTM acrylate medical adhesives (CosMED):octyldodecyl lactate:glycerin:sodium hyaluronan. The rationale supporting this mechanism is that the concentrated antigen on the patch surface generates a high concentration gradient of antigen, thereby producing the driving force to promote substance penetration. We previously conducted a clinical study with a hydrogel patch containing TT/DT and confirmed the safety and efficacy in humans (Table 1) [33].

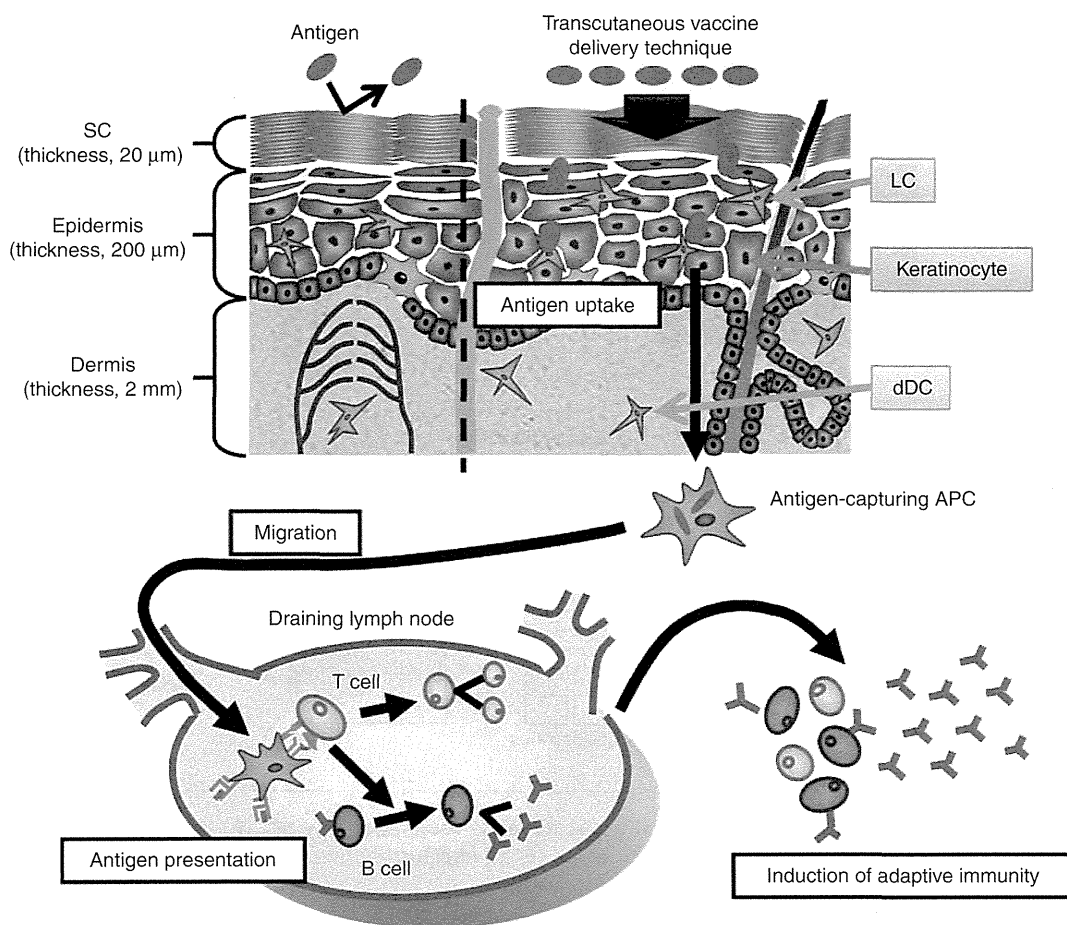


Figure 1. The induction mechanism of immune responses by a transcutaneous vaccine delivery technique.

The disadvantage of using the patch system is the requirement for large quantities of antigen, because each 2 mg TT/DT was applied in our clinical study and the amount of antigen penetrating the skin was a few percentage of the antigen applied to the skin in rats. Finding a suitable adjuvant for TCI to reduce the dose of antigen is also an important factor for the practical use of transcutaneous vaccination using the patch.

3.1.2 Nanoparticles

Nanoparticles are promising entities as antigen carriers for transcutaneous vaccination because of the nano-bio interaction with skin lipids, and the consequent induction of transient and reversible openings in SC [34]. In addition, nanoparticle vaccines can penetrate hair follicles where there is a high density of APCs, target the carried antigens toward APCs and increase the immune response [34-36]. Another advantage is the possibility of encapsulating both the antigen and adjuvant in the same particle, which is suggested to enhance the immune response [37].

The most common nanoparticles have been prepared using polylactic acid (PLA) or/and poly (lactic-co-glycolic

acid) [38]. Fluorescence-labeled nanoparticles were detected in the duct of hair follicles, indicating that nanoparticles can penetrate the skin barrier through hair follicles. Although ovalbumin (OVA)-loaded PLA nanoparticles elicited lower antibody responses than OVA in aqueous solution, they were more efficient at cytokine induction [39]. Chitosan is currently being explored as a biomimetic material for the development of drug delivery systems. Its biodegradability, biocompatibility, low toxicity and simple and mild preparation methods make it an attractive candidate [40,41]. Several reports have indicated that the antigen is protected from degradation by conjugation with the chitosan nanoparticle. The chitosan nanoparticle may act as an adjuvant by functioning as a depot and being more efficiently taken up by dendritic cells than plain antigens because their size and structure are similar to those of microorganisms [42-44].

3.1.3 Elastic vesicles

As mentioned above, formulation of antigens in particulate carriers is popular in vaccine delivery. Recently, elastic

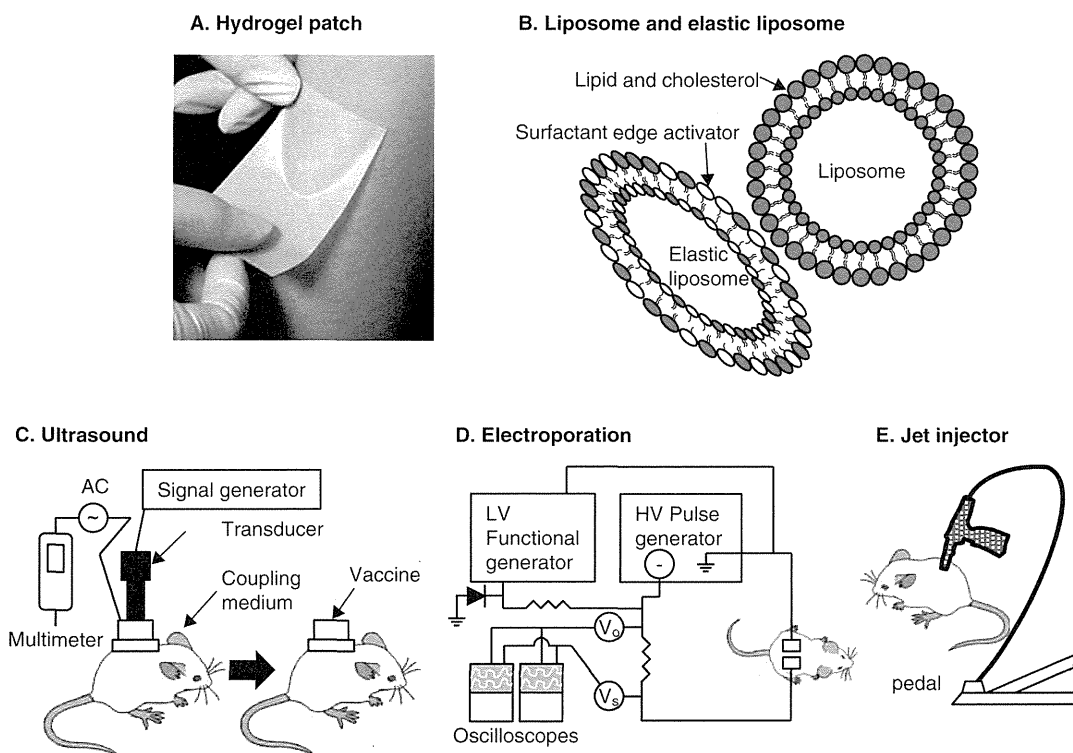


Figure 2. Schematic illustration and photographs of transcutaneous vaccination devices. (A) Hydrogel patch; **(B)** liposome and elastic liposome; **(C)** ultrasound; **(D)** electroporation and **(E)** jet injector.

Table 1. Clinical studies of transcutaneous vaccine delivery.

Formulation or device	Vaccine	Phase	Dose	Company	Refs.
<i>Patch</i>					
SPS	LT for travelers' diarrhea	III	37.5 μ g	IOMAI/	[24]
	Trivalent inactivated seasonal influenza	II	45 μ g LT	Intercell	[25]
CSSS	Inactivated influenza/tetanus or subunit influenza	I	15 μ g		[27,28]
	Melanoma or HIV epitopes	I	4 – 16 mg		[26]
Hydrogel patch	TT/DT	clinical study	2 mg each	CoSMED	[33]
<i>Jet injector</i>					
PMED TM (Powder)	Influenza DNA	I	1 – 4 μ g	Pfizer	[66,70]
	DNA melanoma gp100	I	0.5 – 1 μ g		[68]
	Malaria DNA	I	2.5 mg		[71,72]
Biojector [®] (Liquid)	HIV DNA	I	1 mg	Bioject	[74]
	Inactivated hepatitis A	I	1440 EL. U		[73]
<i>Microneedle</i>					
MicronJet [®]	Trivalent seasonal influenza HA	I	3 – 6 μ g	NanoPass	[96]

CSSS: Cyanoacrylate skin surface stripping; DT: Diphtheria toxoid; HA: hemagglutinin; LT: *Escherichia coli* heat-labile toxin; PMED: Particle-mediated epidermal delivery; SPS: Skin preparation system; TT: Tetanus toxoid.

vesicles, which have a flexible bilayer composed of phospholipid, surfactant and water, have been used as they are thought to penetrate SC more easily compared to conventional liposomes (Figure 2B). With a similar structure to biological membranes, transfersomal systems, including deformable

liposomes and niosomes, have been formulated for the topical/transdermal delivery of bioactive compounds, such as antibiotics, proteins and nucleic acids.

Transfersomes[®] are ultra-deformable liposomes generated by incorporation of a surfactant into the lipid bilayer [45]. The use

of Transfersomes to formulate antigens in TCI has been reported in a few studies. When antigens, such as human serum albumin, gap junction protein or TT are used, potent humoral immune responses are induced in murine models with antibody levels comparable to those obtained through subcutaneous injection [46-48]. Variants of elastic vesicles have also been evaluated in TCI, such as ethosomes, which have a high percentage of ethanol introduced into the vesicles, or niosomes, which are constructed from nonionic surfactants and cholesterol. TCI of hepatitis B surface antigen (HBsAg)-loaded ethosomes (composed of soya phosphatidylcholine and ethanol) has been reported to induce an immune response comparable to intramuscular injection of HBsAg-alum [49]. Bovine serum albumin (BSA)-loaded niosomes, composed of Span 60, Span 85, cholesterol and stearylamine, were coated with a modified polysaccharide, O-palmitoyl mannan, for targeted delivery to LCs. This niosomal formulation elicited significantly higher serum IgG titers compared to alum-adsorbed BSA or plain uncoated niosomes in TCI, but the titers were still lower than those obtained after intramuscular injection of an equivalent dose of BSA-alum [50]. Thereafter, the optimization of niosomes with respect to the composition or dose is needed for improving efficacy and practical use.

3.2 Physical techniques for TCI

Many studies have reported that topical application of the vaccine formulation alone cannot yield an adequate immune response. This creates an attractive challenge for developing physical methods to overcome SC.

3.2.1 Ultrasound

Low-frequency ultrasound (Figure 2C) is known to increase the skin permeation of large molecules and enable transcutaneous vaccination. Ultrasonic TCI offers a needle-free and painless immunization and can increase anti-TT antibody titer [51]. The use of ultrasound can be defined as a physical adjuvant for TCI because slight LC activation was observed after ultrasound in the absence of antigen [52]. Low-frequency ultrasound application to the skin is known to extract skin lipids, cause the formation of defects and lacunar spaces within the skin and create highly permeable localized transport regions in the skin. Thus, liposome application to sonicated skin could allow/enhance liposome/antigen flux into the skin and consequently enhance TCI. Liposome application repaired the skin damage caused by ultrasound, although greater damage caused by skin sonication in the presence of sodium dodecyl sulfate was not repaired [53]. This suggests that synergistic effects between liposomes and ultrasound for TCI may be possible. However, it should be considered that vaccination by ultrasound requires the use of bulky, specialized equipment.

3.2.2 Electroporation

Increased molecular transport results from structural rearrangements to the cell membrane [54]. Electroporation

(Figure 2D) results in transient structural perturbation of lipid bilayer membranes, including SC, in response to high-voltage pulses. This technique extends the transfection efficiency to many skin cells [55,56]. Previously, electroporation was widely used as a transcutaneous drug delivery system. Compared to injection, electroporation is less invasive because of the new availability of noninvasive probes. A study has shown that exodus of LCs from the skin was stimulated, and the OVA-specific CTL response to the vaccine delivered by needle-free electroporation was equivalent to that of intradermal injection [57]. Efficient priming of immune responses by human immunodeficiency virus DNA electroporation in conjunction with a protein boost may give rise to long-term immunity [58,59]. However, similar to ultrasound, the electroporation technique requires a specialized device.

3.2.3 Jet injector

The jet injector (Figure 2E) delivers powder or liquid antigen into the skin by air pressure using compressed helium [60-62]. Many studies have been conducted using epidermal powder immunization, showing protective immune responses against influenza, hepatitis B and DT, with doses ranging from 0.2 to 5 µg [63,64]. This device has been acquired by Pfizer (particle-mediated epidermal delivery; PMED™) to target dry powder DNA vaccines, primarily to the epidermis of the skin (Table 1) [65-72]. The disruption by this system causes mild side effects, such as application-site burning, which usually resolves within hours [66,70]. On the other hand, Biojector® has been developed as a liquid jet injector by Bioject (Table 1) [73,74]. A higher proportion of people who received the hepatitis A DNA vaccine using Biojector as a liquid jet injector seroconverted with hepatitis A virus compared with vaccination using an injection [73]. Although hand-size device was developed and handling of device was to be easy-to-use, jet injector is poor method in prevalence of vaccination because of the strong pain.

3.2.4 Microneedle

The most widely used method to overcome the skin barrier is intradermal injection, which enables precise and reproducible delivery of antigens into the dermis. Some studies reported that the efficacy of influenza intradermal injection was greater than that of conventional intramuscular injection, suggesting that vaccination targeting the skin is promising [75,76]. However, traditional intradermal injection requires well-trained healthcare workers, which has led to the development of new devices for intradermal injection. One example is the Becton Dickinson (BD) microinjection system, Soluvia™ [77,78]. This is a prefilled syringe with a single 1.5 mm long, 30 G intradermal needle designed to deliver 100 – 200 µL fluid. It is now commercially available for a trivalent seasonal influenza vaccine (Sanofi-Pasteur) [79]. These studies underline the effectiveness of the skin as an immunization site, but intradermal injection still employs the use of long needles and is painful. A minimally invasive means of vaccinating healthy people by TCI is desirable.

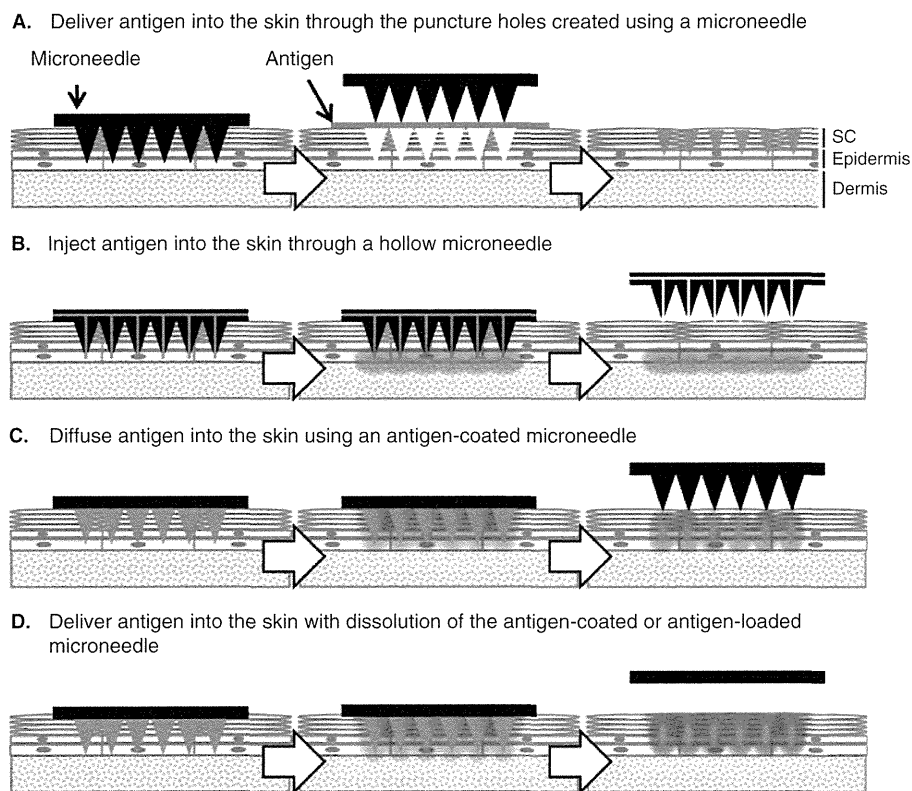


Figure 3. Examples of transcutaneous delivery using microneedle. (A) Solid microneedle; (B) hollow microneedle; (C) coated microneedle and (D) dissolving microneedle.

One approach toward painless TCI is to dramatically reduce the needle size so that they are barely perceptible. The concept of the microneedle array for drug delivery essentially dates back to a patent, filed in 1976, by Gerstel and Place [80]. However, it was not until the 1990s that the technique became viable, as by this time, fabrication techniques had become available to produce these microneedle arrays in a potentially cost-effective manner.

In this context, the term ‘microneedle’ refers to needles shorter than 1 mm. Microneedles only need to pierce the 15 to 20 μm thick SC before reaching the viable epidermis. However, the skin is an elastic, heterogeneous tissue and is slightly stretched *in vivo*. The mechanical and structural properties of the skin significantly vary with age, skin type, hydration level, body location and among individuals [81]. To ensure effective and reproducible piercing regardless of these factors, microneedles need to be much longer than 20 μm [82]. Other parameters, such as microneedle diameter, insertion depth, microneedle tip geometry and microneedle density also influence skin perforation and antigen delivery [82–84]. For instance, very thin microneedles are fragile, which results in an increased risk of fracture in the skin [85]. In addition, increased microneedle density can give rise to the ‘bed of nails’ effect and does not improve antigen delivery [82].

Various strategies using microneedle technology were developed for transdermal drug delivery, including TCI [86–88], because microneedle approach is one of the most easy-to-use methods by just applying it on the skin. The important strategies are summarized below (Figure 3).

3.2.4.1 Solid microneedles

The first method using microneedles involves perforation of the skin with solid microneedle arrays and application of antigens to the skin surface for subsequent diffusion into the skin (Figure 3A). Henry *et al.* demonstrated a four-order-of-magnitude increase in permeability for calcein and BSA through human epidermis *in vitro* after penetration with a microneedle array of 150 μm long needle [89]. Banks *et al.* reported that the flux across the microneedle array pretreated skin was augmented by increasing the charge of the drug [90]. In addition, it was reported that 200 nm particles can diffuse through conduits formed by a solid microneedle array (300 μm long, 4 \times 4 array), which was applied at a speed of 3 m/s using an electric applicator [91]. In the absence of such an applicator, no conduits were formed. In the efficacy assessment of TCI, pretreatment of the skin using the same type of microneedle array led to a 1,000-fold increase in antibody titer after

topical application of DT in mice [92]. The immune response was further boosted by co-application of cholera toxin (CT), suggesting that selective addition of adjuvants may lower the antigen dose required [93]. A 3M has developed the micro-structured transdermal system using coated or uncoated solid microneedles. In collaboration with VaxInnate, these microneedles will be used for the delivery of an influenza vaccine.

As a variant of the treatment using solid microneedles, a post-treatment method was developed [94]. The skin was painted with a vaccine solution and then gently scraped by microneedles to expose the epidermis to the vaccine without causing pain sensation. Using BD's OnVax[®] device, which has a microneedle length ranging from 50 to 200 μm over a 1 cm^2 area, stronger and less variable immune responses were achieved compared to intramuscular and intradermal injection with the same dose of hepatitis B DNA vaccine (100 μg). Moreover, 100% seroconversion was achieved after only two vaccinations, whereas only 40 – 50% conversion was obtained by intramuscular injection.

In general, pre- or post-treatment with the microneedle array is considered a simple approach for TCI that has great potential, but parameters such as dose and application time should be optimized.

3.2.4.2 Hollow microneedles

During pretreatment with a solid microneedle array, antigen delivery is dependent on passive diffusion along the conduits created by the microneedles. Although this is a relatively easy approach from a technical point of view, it is difficult to optimize the antigen quantity required to activate immune cells in the skin because of limited transport through the conduits. Hollow microneedle arrays can inject the vaccine to a well-defined depth in the skin by precisely steering the flow rate using a syringe or a pump (Figure 3B).

Hollow microneedles are made of various materials, such as silicon, metal and glass [95]. Recently, the potential of hollow microneedles for vaccination has received attention as it can be used for both TCI and intradermal vaccination depending on the microneedle length. Influenza vaccination (3.3 μg of hemagglutinin [HA] per strain) using a hollow microneedle array (450 μm long, 4 \times 1, MicronJet developed by Nanopass) induced immune responses similar to those induced by intramuscular injection of 15 μg HA per strain to human volunteers (Table 1) [96].

The main technical demands are avoiding leakage and clogging of the microneedles during injection. Whereas clogging can be prevented using a beveled tip [83], the short-length needle increases the chance for leakage. Therefore, optimization of the flow rate, needle length and localization of the opening are demanded. In addition, the hollow microneedle formulation has the disadvantage of requiring cold chain storage and transportation of antigen solutions in addition to the injection system.

3.2.4.3 Coated microneedles

Microneedle arrays precoated (Figure 3C) with 1 μg OVA induced a 100-fold increase in immune response compared to intramuscular injection of the same dose [97]. The titanium microneedles in the array were 300 μm long and were applied to the skin using an impact insertion applicator. Furthermore, an extensive study was conducted on the influence of OVA-coated microneedle properties on the immune response. The immune response was found to be dose-dependent, but practically independent of depth of delivery, density of microneedles or area of application. Interestingly, OVA vaccination with short microneedles (225 μm) in a high-density array (725 microneedles/ cm^2) induced an immune response similar to that induced by longer microneedles (600 μm) in a low-density array (140 microneedles/ cm^2) [82]. This led to the development of the macroflux system, which is now undergoing a Phase I clinical study for TCI with an influenza vaccine. Efficacy using coated microneedles was reported for various antigens including OVA, H3N2 influenza antigen, inactivated influenza virus and hepatitis C DNA.

Coatings are usually applied by dipping the microneedle into a vaccine formulation [98,99]. Another method is to use gas jet coating to achieve a more uniform coating of densely packed microneedles [100]. Coated microneedle arrays may not be very attractive for transdermal drug delivery as only a limited quantity of active compounds can be coated onto the microneedle. However, this quantity might be sufficient for antigens to elicit a protective immune response. In addition, one of the advantages of coated microneedles is that dried antigen adhered to the surface of the microneedles may improve the long-term stability [101]. It was reported that coating reduced the immunogenicity of the vaccine, thus requiring trehalose to partially retain the activity [102,103].

A method of combining coated microneedles with electroporation has been developed [104]. The EasyVaxTM device inserts coated microneedle arrays into the skin, followed by electrical pulses, to deliver DNA into the cells. Neutralizing antibody titers induced by TCI with a smallpox DNA vaccine using this system were greater than those induced by the traditional live virus vaccine administered by scarification. However, the main drawback of this approach for practical use is the complexity of the device.

3.2.4.4 Dissolving microneedles

Conventional microneedles suffer from the risk of fracture, which might leave metals, stainless steel or silicon microneedle fragments in the skin. The use of dissolvable or biodegradable materials containing vaccine components is an elegant way to deliver a vaccine without the possibility of microneedles breaking off in the skin (Figure 3D). Moreover, dissolving microneedles leave no biohazardous sharp medical waste and remove the risk of secondary infection by used needles.

The first microneedles were made of maltose [105] and later, development of dextrin microneedle array was reported for the delivery of insulin and erythropoietin [106,107]. Recently,

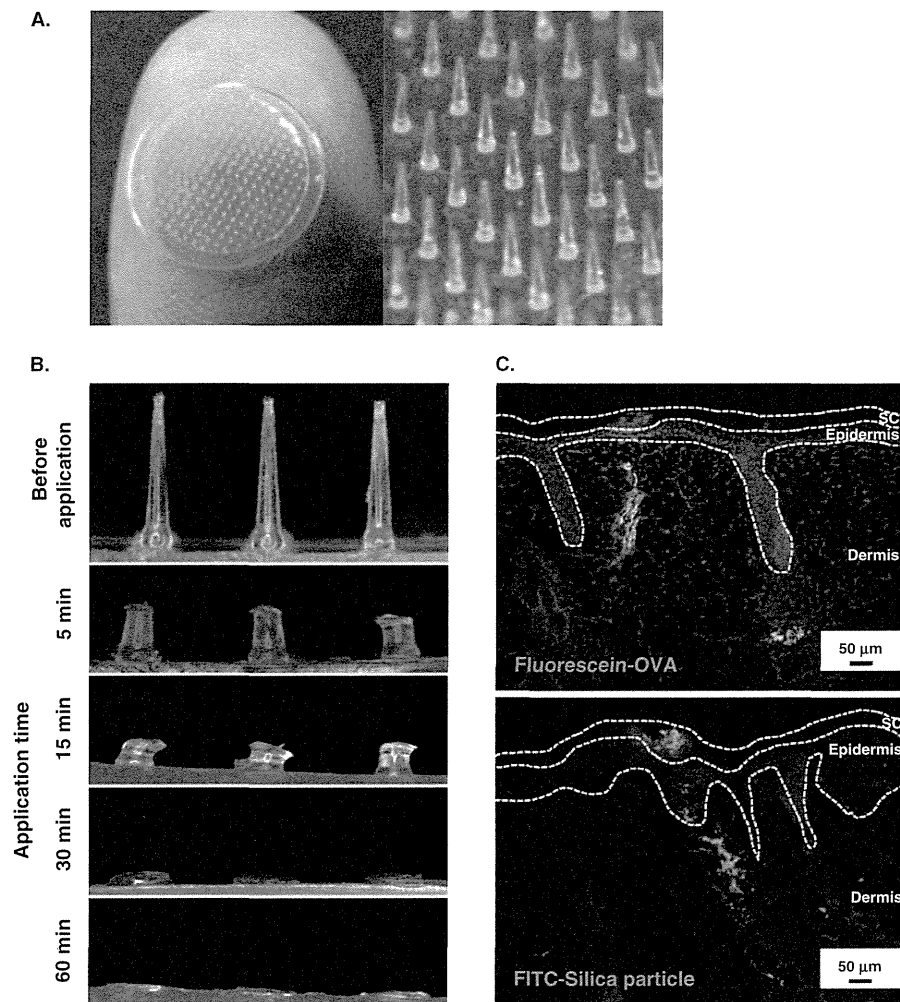


Figure 4. Photographs of MH and observation of microneedles and skin after MH application. (A) MH is made of hyaluronic acid and contains 200 microneedles/ patch (0.8 cm²). (B) MH of 800 μm long needle were applied to the back skin of Wistar ST rats for the indicated times. After removal of MH, the microneedles remaining on MH were photographed using a stereoscopic microscope. (C) Fluorescein-OVA (green) or FITC-silica particle (green)-containing MH of 800 μm long needle were applied to the back skin of Wistar ST rats for 6 h. The skin was harvested and frozen. Frozen sections (6 μm thick) were photographed under a fluorescence microscope. The nucleus was counterstained using DAPI (blue).

Sullivan *et al.* showed that immunization with polymeric dissolving microneedles containing inactivated influenza virus induced a strong antibody and cellular response and provided protection against challenge by influenza [108]. The manufacture of dissolving microneedles requires technical expertise to allow the antigen to be incorporated into the matrix of the microneedle material using mild procedures that do not cause antigen breakdown or compromise material strength. The high temperatures required to mold polymers led to significant drug loss. The microneedles used by Sullivan *et al.* are made by a photo-polymerization method, which uses UV light to form microneedles without compromising β-galactosidase activity. Companies, such as

Theraject and BioSerenTach, are currently developing dissolving microneedle systems for vaccine delivery. The Theraject VaxMAT, made of a sugar matrix containing vaccine components, is fabricated in various lengths from 100 to 1,000 μm and is assembled with an adhesive patch. After application, the microneedles dissolve and the antigen diffuses into the epidermis and dermis within a few minutes.

We have developed a self-dissolving microneedle patch (MicroHyla[®]; MH) made of biocompatible hyaluronic acid (Figure 4A) [109,110]. Our MH was prepared in various lengths from 200 to 800 μm and in two shapes of microneedle; konide and cone [109]. Sixty minutes after application, the microneedles had dissolved completely and delivered both

Table 2. Development of adjuvants for transcutaneous vaccination.

Transcutaneous adjuvant	Antigen	Immune response	Refs.
CT, CTB	DT	IgG	[111]
	TT	IgG	[111]
	OVA	IgG, IgG2a, CTL, CD4 ⁺	[115,116]
LT	Influenza	IgG, IgG1, CD4 ⁺	[113,114]
	TT	IgG, IgG1	[112]
Imiquimod	OVA	CTL	[121]
CpG ODN	TT	IgG, IgG2a	[112]
	Influenza	IgG2a, CD4 ⁺	[113,114]

CT: Cholera toxin; CTB: B subunit of cholera toxin; CTL: Cytotoxic T cell; DT: Diphtheria toxoid; LT: *Escherichia coli* heat-labile toxin; ODN: Oligodeoxynucleotide; OVA: Ovalbumin; TT: Tetanus toxoid.

soluble and particulate material into the skin (Figure 4B and 4C). We previously reported that TCI using MH effectively induced immune responses against various antigens in animal models, and furthermore, the application of MH resulted in minimal skin irritation in rats [110]. Moreover, we conducted a clinical study to assess the safety of the MH device in humans and showed that our new MH is a practical and safe device for use in human immunization. A clinical study using influenza HA antigen-containing MH is in progress, and we have confirmed that TCI using MH induced immune responses without severe side effects (unpublished data).

4. Adjuvant development for TCI

In TCI, the co-application of adjuvants with the antigen is required for induction of a strong immune response. Aluminum hydroxide hydrate and Freund's adjuvant are commonly used as immune adjuvants. However, these adjuvants are not useful in TCI because their relatively large sizes do not permit skin penetration. Adjuvants for TCI can be divided into bacterial enterotoxin and toll-like receptor (TLR) ligands (Table 2).

4.1 Bacterial enterotoxins

Bacterial enterotoxins have high adjuvant activity and are most often used preclinically for TCI. CT and LT are the most intensively studied [73]. CT and LT not only produce anti-CT and anti-LT antibodies but also improve the total immune response and affect the quality of the immune response (Table 2) [111-114]. In addition to antibody responses, it was shown that CT can induce a CTL response [115] and that A and B subunits of CT (CTA and CTB) are responsible for the expression of different cytokines from restimulated lymphocytes isolated from the spleens of immunized mice [116]. However, the safety cannot be assured because LT or CT, which are toxins, can cause excessive tissue injury or necrosis. Difficulties have been encountered applying the toxin to the human skin, and additional studies are required to elucidate how toxins affect immune responses.

4.2 TLR ligands

TLRs are important signal molecules when cells sense danger [117] and are expressed on the surface of LCs, dDCs and keratinocytes. Therefore, purified or synthetic TLR ligands are expected to be suitable adjuvants for vaccination purposes [118,119]. One example is imiquimod, which is a ligand for TLR7 and TLR8. Imiquimod induced migration of LCs and resulted in the production of IFN- α and TNF- α (Table 2) [120-122]. Another ligand is cytosine-phosphate-guanine (CpG) oligodeoxynucleotide (ODN). By signaling through TLR9, CpG ODN enhanced the vaccine's immunogenicity and induced antibody production and proinflammatory cytokines, such as TNF- α and IFN- γ [113,114]. Various TLR ligands are currently being developed as effective adjuvants for practical use.

5. Conclusion

The skin is an important immunological site and has the potential to be an ideal non- or low-invasive vaccination site, although it possesses a complex barrier. TCI provides effective, easy-to-use and painless vaccination with little side effect and safer handling than conventional injections. The main challenges of TCI are ensuring accurate delivery of antigens into the epidermal or dermal skin tissue where LCs and dDCs are present, and to activate specific immune response. Many different approaches have been developed of which several ways may lead to successful TCI, and clinical studies of some devices have been conducted. However, satisfactory guidelines about the standard for formulation and evaluation of safety and efficacy have not yet been regulated because of the novelty of this formulation. Various information about the characteristics of skin as a target and the fundamental properties of TCI devices may lead to the establishment and refinement of guidelines for TCI formulation. Such guidelines will encourage researchers and pharmaceutical companies to develop practical TCI systems.

6. Expert opinion

Many strategies, in particular microneedle devices [123-125], have been developed for TCI systems. Such strategies could be easy-to-use methods of vaccination. For the practical use of these TCI formulations, the safety and efficacy of TCI must be confirmed. Therefore, knowing the function of immunocytes, such as APCs, T cells, macrophages and keratinocytes, in the skin is important. Analysis of the immunological characteristics of each type of cell (e.g., surface marker expression and cytokine production) can help elucidate the molecular and/or cellular mechanisms that underlie the immunity of the skin. In addition, recent studies using two-photon confocal microscopy or genetically modified mice have enabled direct observation of the kinetics and distribution of immune cells in the skin and the interaction between APCs and T cells in draining lymph nodes and

have lead to understand skin immunity *in vivo* [126,127]. Such studies are useful for the development/improvement of transcutaneous vaccination formulations and can guarantee the safety and efficacy of TCI systems. Moreover, transcutaneous delivery of adjuvant is required for more effective immune responses, the reduction of antigen dose and/or number of administrations and the expansion of applications to various diseases. Advances in understanding the functional properties of immunocytes in the skin contribute to the development of adjuvants suitable for TCI by providing information on the delivery target of antigen and adjuvant. Thus, if the bias of immune responses can be controlled by the appropriate selection of TCI methods and/or adjuvants, TCI systems could be used to create strategies against Alzheimer's disease, autoimmune diseases and cancer. Basic scientific research must be actively evolved to the translational research to assess

application of TCI systems to human. We believe that the practical use is achieved early by promoting the consistent studies from basic research to clinical trial led by TCI researchers including us.

Declaration of interest

Our studies mentioned in this review were conducted in collaboration with CosMED Pharmaceuticals Co. Ltd., Nara Medical University, Osaka University Graduate School of Medicine, and The Research Foundation for Microbial Diseases of Osaka University. Our work was supported by the National Institute of Biomedical Innovation (NIBIO), the Ministry of Health, Labour and Welfare, and the Ministry of Education, Culture, Sports, Science and Technology of Japan.

Bibliography

Papers of special note have been highlighted as either of interest (●) or of considerable interest (●●) to readers.

- Leppin A, Aro AR. Risk perceptions related to SARS and avian influenza: theoretical foundations of current empirical research. *Int J Behav Med* 2009;16:7-29
- Haque A, Lucas B, Hober D. Influenza A/H5N1 virus outbreaks and preparedness to avert flu pandemic. *Ann Biol Clin (Paris)* 2007;65:125-33
- Valadas E, Antunes F. Tuberculosis, a re-emergent disease. *Eur J Radiol* 2005;55:154-7
- Campbell CC. Malaria: an emerging and re-emerging global plague. *FEMS Immunol Med Microbiol* 1997;18:325-31
- Jones JH, Salathe M. Early assessment of anxiety and behavioral response to novel swine-origin influenza A(H1N1). *PLoS One* 2009;4:e8032
- Azad N, Rojanasakul Y. Vaccine delivery—current trends and future. *Curr Drug Deliv* 2006;3:137-46
- Kersten G, Hirschberg H. Needle-free vaccine delivery. *Expert Opin Drug Deliv* 2007;4:459-74
- UNICEF's work on immunisation. Available from: <http://www.unicef.org.uk/UNICEFs-Work/What-we-do/UNICEFs-work-on-immunisation/>
- Glenn GM, Scharon-Kersten T, Alving CR. Advances in vaccine delivery: transcutaneous immunisation. *Expert Opin Investig Drugs* 1999;8:797-805
- Levine MM. Can needle-free administration of vaccines become the norm in global immunization? *Nat Med* 2003;9:99-103
- Mathers AR, Larregina AT. Professional antigen-presenting cells of the skin. *Immunol Res* 2006;36:127-36
- Metz M, Siebenhaar F, Maurer M. Mast cell functions in the innate skin immune system. *Immunobiology* 2008;213:251-60
- Sugita K, Kabashima K, Atarashi K, et al. Innate immunity mediated by epidermal keratinocytes promotes acquired immunity involving Langerhans cells and T cells in the skin. *Clin Exp Immunol* 2007;147:176-83
- Mutyambizi K, Berger CL, Edelson RL. The balance between immunity and tolerance: the role of Langerhans cells. *Cell Mol Life Sci* 2009;66:831-40
- Nestle FO, Nickoloff BJ. Deepening our understanding of immune sentinels in the skin. *J Clin Invest* 2007;117:2382-5
- Valladeau J, Saeland S. Cutaneous dendritic cells. *Semin Immunol* 2005;17:273-83
- Gockel CM, Bao S, Beagley KW. Transcutaneous immunization induces mucosal and systemic immunity: a potent method for targeting immunity to the female reproductive tract. *Mol Immunol* 2000;37:537-44
- Rougier A, Ralliss M, Krien P, et al. In vivo percutaneous absorption: a key role for stratum corneum/vehicle partitioning. *Arch Dermatol Res* 1990;282:498-505
- Bos JD, Meinardi MM. The 500 Dalton rule for the skin penetration of chemical compounds and drugs. *Exp Dermatol* 2000;9:165-9
- Barry BW. Breaching the skin's barrier to drugs. *Nat Biotechnol* 2004;22:165-7
- Glenn GM, Villar CP, Flyer DC, et al. Safety and immunogenicity of an enterotoxigenic *Escherichia coli* vaccine patch containing heat-labile toxin: use of skin pretreatment to disrupt the stratum corneum. *Infect Immun* 2007;75:2163-70
- McKenzie R, Bourgeois AL, Frech SA, et al. Transcutaneous immunization with the heat-labile toxin (LT) of enterotoxigenic *Escherichia coli* (ETEC): protective efficacy in a double-blind, placebo-controlled challenge study. *Vaccine* 2007;25:3684-91
- Glenn GM, Taylor DN, Li X, et al. Transcutaneous immunization: a human vaccine delivery strategy using a patch. *Nat Med* 2000;6:1403-6
- Frech SA, Dupont HL, Bourgeois AL, et al. Use of a patch containing heat-labile toxin from *Escherichia coli* against travellers' diarrhoea: a phase II, randomised, double-blind, placebo-controlled field trial. *Lancet* 2008;371:2019-25
- **Wide-scale clinical trial of transcutaneous vaccination.**
- Frech SA, Kenney RT, Spyr CA, et al. Improved immune responses to influenza vaccination in the elderly using an

- immunostimulant patch. *Vaccine* 2005;23:946-50
26. Yagi H, Hashizume H, Horibe T, et al. Induction of therapeutically relevant cytotoxic T lymphocytes in humans by percutaneous peptide immunization. *Cancer Res* 2006;66:10136-44
27. Vogt A, Mahe B, Costagliola D, et al. Transcutaneous anti-influenza vaccination promotes both CD4 and CD8 T cell immune responses in humans. *J Immunol* 2008;180:1482-9
28. Combadiere B, Vogt A, Mahe B, et al. Preferential amplification of CD8 effector-T cells after transcutaneous application of an inactivated influenza vaccine: a randomized phase I trial. *PLoS One* 2010;5:e10818
29. Ishii Y, Nakae T, Sakamoto F, et al. A transcutaneous vaccination system using a hydrogel patch for viral and bacterial infection. *J Control Release* 2008;131:113-20
30. Matsuo K, Ishii Y, Quan YS, et al. Transcutaneous vaccination using a hydrogel patch induces effective immune responses to tetanus and diphtheria toxoid in hairless rat. *J Control Release* 2011;149:15-20
31. Matsuo K, Ishii Y, Quan YS, et al. Compositional optimization and safety assessment of a hydrogel patch as a transcutaneous immunization device. *Biol Pharm Bull* 2011;34:1835-40
32. Matsuo K, Ishii Y, Quan YS, et al. Characterization of transcutaneous protein delivery by a hydrogel patch in animal, human, and tissue-engineered skin models. *Biol Pharm Bull* 2011;34:586-9
33. Hirobe S, Matsuo K, Quan YS, et al. Clinical study of transcutaneous vaccination using a hydrogel patch for tetanus and diphtheria. *Vaccine* 2012;30:1847-54
34. Kohli AK, Alpar HO. Potential use of nanoparticles for transcutaneous vaccine delivery: effect of particle size and charge. *Int J Pharm* 2004;275:13-17
35. Shaker DS, Sloar BR, Le UM, et al. Immunization by application of DNA vaccine onto a skin area wherein the hair follicles have been induced into anagen-onset stage. *Mol Ther* 2007;15:2037-43
36. Vogt A, Combadiere B, Hadam S, et al. 40 nm, but not 750 or 1,500 nm, nanoparticles enter epidermal CD1a+ cells after transcutaneous application on human skin. *J Invest Dermatol* 2006;126:1316-22
37. Schlosser E, Mueller M, Fischer S, et al. TLR ligands and antigen need to be coencapsulated into the same biodegradable microsphere for the generation of potent cytotoxic T lymphocyte responses. *Vaccine* 2008;26:1626-37
38. Panyam J, Labhasetwar V. Biodegradable nanoparticles for drug and gene delivery to cells and tissue. *Adv Drug Deliv Rev* 2003;55:329-47
39. Mattheolabakis G, Lagoumintzis G, Panagi Z, et al. Transcutaneous delivery of a nanoencapsulated antigen: induction of immune responses. *Int J Pharm* 2010;385:187-93
40. Nagpal K, Singh SK, Mishra DN. Chitosan nanoparticles: a promising system in novel drug delivery. *Chem Pharm Bull (Tokyo)* 2010;58:1423-30
41. Prego C, Paolicelli P, Diaz B, et al. Chitosan-based nanoparticles for improving immunization against hepatitis B infection. *Vaccine* 2010;28:2607-14
42. Bal SM, Slutter B, Jiskoot W, et al. Small is beautiful: N-trimethyl chitosan-ovalbumin conjugates for microneedle-based transcutaneous immunisation. *Vaccine* 2011;29:4025-32
43. Bal SM, Slutter B, van Riet E, et al. Efficient induction of immune responses through intradermal vaccination with N-trimethyl chitosan containing antigen formulations. *J Control Release* 2010;142:374-83
44. Bal SM, Ding Z, Kersten GF, et al. Microneedle-based transcutaneous immunisation in mice with N-trimethyl chitosan adjuvanted diphtheria toxoid formulations. *Pharm Res* 2010;27:1837-47
45. El Maghraby GM, Williams AC, Barry BW. Interactions of surfactants (edge activators) and skin penetration enhancers with liposomes. *Int J Pharm* 2004;276:143-61
46. Paul A, Cevc G, Bachhawat BK. Transdermal immunization with large proteins by means of ultradeformable drug carriers. *Eur J Immunol* 1995;25:3521-4
47. Paul A, Cevc G, Bachhawat BK. Transdermal immunisation with an integral membrane component, gap junction protein, by means of ultradeformable drug carriers, transfersomes. *Vaccine* 1998;16:188-95
48. Gupta PN, Mishra V, Rawar A, et al. Non-invasive vaccine delivery in transfersomes, niosomes and liposomes: a comparative study. *Int J Pharm* 2005;293:73-82
49. Mishra D, Mishra PK, Dubey V, et al. Systemic and mucosal immune response induced by transcutaneous immunization using Hepatitis B surface antigen-loaded modified liposomes. *Eur J Pharm Sci* 2008;33:424-33
50. Jain S, Vyas SP. Mannosylated niosomes as carrier adjuvant system for topical immunization. *J Pharm Pharmacol* 2005;57:1177-84
51. Dahlan A, Alpar HO, Strickings P, et al. Transcutaneous immunisation assisted by low-frequency ultrasound. *Int J Pharm* 2009;368:123-8
52. Tezel A, Paliwal S, Shen Z, et al. Low-frequency ultrasound as a transcutaneous immunization adjuvant. *Vaccine* 2005;23:3800-7
53. Dahlan A, Alpar HO, Murdan S. An investigation into the combination of low frequency ultrasound and liposomes on skin permeability. *Int J Pharm* 2009;379:139-42
54. Weaver JC. Electroporation theory. Concepts and mechanisms. *Methods Mol Biol* 1995;55:3-28
55. Prausnitz MR, Bose VG, Langer R, et al. Electroporation of mammalian skin: a mechanism to enhance transdermal drug delivery. *Proc Natl Acad Sci USA* 1993;90:10504-8
56. Vanbever R, Lecouturier N, Preat V. Transdermal delivery of metoprolol by electroporation. *Pharm Res* 1994;11:1657-62
57. Zhao YL, Murthy SN, Manjili MH, et al. Induction of cytotoxic T-lymphocytes by electroporation-enhanced needle-free skin immunization. *Vaccine* 2006;24:1282-90
58. Cristillo AD, Weiss D, Hudacik L, et al. Persistent antibody and T cell responses induced by HIV-1 DNA vaccine delivered by electroporation. *Biochem Biophys Res Commun* 2008;366:29-35

59. Hirao LA, Wu L, Khan AS, et al. Intradermal/subcutaneous immunization by electroporation improves plasmid vaccine delivery and potency in pigs and rhesus macaques. *Vaccine* 2008;26:440-8
60. Macklin MD, McCabe D, McGregor MW, et al. Immunization of pigs with a particle-mediated DNA vaccine to influenza A virus protects against challenge with homologous virus. *J Virol* 1998;72:1491-6
61. Chen D, Zuleger C, Chu Q, et al. Epidermal powder immunization with a recombinant HIV gp120 targets Langerhans cells and induces enhanced immune responses. *AIDS Res Hum Retroviruses* 2002;18:715-22
62. Kelly K, Loskutov A, Zehring D, et al. Preventing contamination between injections with multiple-use nozzle needle-free injectors: a safety trial. *Vaccine* 2008;26:1344-52
63. Chen D, Weis KF, Chu Q, et al. Epidermal powder immunization induces both cytotoxic T-lymphocyte and antibody responses to protein antigens of influenza and hepatitis B viruses. *J Virol* 2001;75:11630-40
64. Chen D, Endres R, Maa YF, et al. Epidermal powder immunization of mice and monkeys with an influenza vaccine. *Vaccine* 2003;21:2830-6
65. Roberts LK, Barr LJ, Fuller DH, et al. Clinical safety and efficacy of a powdered Hepatitis B nucleic acid vaccine delivered to the epidermis by a commercial prototype device. *Vaccine* 2005;23:4867-78
66. Drape RJ, Macklin MD, Barr LJ, et al. Epidermal DNA vaccine for influenza is immunogenic in humans. *Vaccine* 2006;24:4475-81
67. Dincer Z, Jones S, Haworth R. Preclinical safety assessment of a DNA vaccine using particle-mediated epidermal delivery in domestic pig, minipig and mouse. *Exp Toxicol Pathol* 2006;57:351-7
68. Cassaday RD, Sondel PM, King DM, et al. A phase I study of immunization using particle-mediated epidermal delivery of genes for gp100 and GM-CSF into uninvolved skin of melanoma patients. *Clin Cancer Res* 2007;13:540-9
69. Braun RP, Dong L, Jerome S, et al. Multi-antigenic DNA immunization using herpes simplex virus type 2 genomic fragments. *Hum Vaccin* 2008;4:36-43
70. Jones S, Evans K, McElwaine-Johnn H, et al. DNA vaccination protects against an influenza challenge in a double-blind randomised placebo-controlled phase 1b clinical trial. *Vaccine* 2009;27:2506-12
71. Wang R, Epstein J, Baraceros FM, et al. Induction of CD4(+) T cell-dependent CD8(+) type 1 responses in humans by a malaria DNA vaccine. *Proc Natl Acad Sci USA* 2001;98:10817-22
72. Epstein JE, Gorak EJ, Charoenvit Y, et al. Safety, tolerability, and lack of antibody responses after administration of a PfCSP DNA malaria vaccine via needle or needle-free jet injection, and comparison of intramuscular and combination intramuscular/intradermal routes. *Hum Gene Ther* 2002;13:1551-60
73. Williams J, Fox-Leyva L, Christensen C, et al. Hepatitis A vaccine administration: comparison between jet-injector and needle injection. *Vaccine* 2000;18:1939-43
74. Aboud S, Nilsson C, Karlen K, et al. Strong HIV-specific CD4+ and CD8+ T-lymphocyte proliferative responses in healthy individuals immunized with an HIV-1 DNA vaccine and boosted with recombinant modified vaccinia virus ankara expressing HIV-1 genes. *Clin Vaccine Immunol* 2010;17:1124-31
75. Belshe RB, Newman FK, Cannon J, et al. Serum antibody responses after intradermal vaccination against influenza. *N Engl J Med* 2004;351:2286-94
- **Benefit of transcutaneous vaccination.**
76. Kenney RT, Frech SA, Muenz LR, et al. Dose sparing with intradermal injection of influenza vaccine. *N Engl J Med* 2004;351:2295-301
- **Benefit of transcutaneous vaccination.**
77. BD Soulvia™ Prefillable Microinjection System. Available from: <http://www.bd.com/pharmaceuticals/products/microinjection.asp>
78. Laurent PE, Bonnet S, Alchas P, et al. Evaluation of the clinical performance of a new intradermal vaccine administration technique and associated delivery system. *Vaccine* 2007;25:8833-42
79. Prymula R, Usluer G, Altinel S, et al. Acceptance and opinions of Intanza/IDflu intradermal influenza vaccine in the Czech Republic and Turkey. *Adv Ther* 2012;29:41-52
80. Gerstel MS, Place VA. Drug delivery device. US Patent No. 3 1976;964:482
81. Reihnsner R, Balogh B, Menzel EJ. Two-dimensional elastic properties of human skin in terms of an incremental model at the in vivo configuration. *Med Eng Phys* 1995;17:304-13
82. Widera G, Johnson J, Kim L, et al. Effect of delivery parameters on immunization to ovalbumin following intracutaneous administration by a coated microneedle array patch system. *Vaccine* 2006;24:1653-64
83. Martanto W, Moore JS, Kashlan O, et al. Microinfusion using hollow microneedles. *Pharm Res* 2006;23:104-13
84. Martanto W, Moore JS, Couse T, et al. Mechanism of fluid infusion during microneedle insertion and retraction. *J Control Release* 2006;112:357-61
85. Davis SP, Landis BJ, Adams ZH, et al. Insertion of microneedles into skin: measurement and prediction of insertion force and needle fracture force. *J Biomech* 2004;37:1155-63
86. Donnelly RF, Raj Singh TR, Woolfson AD. Microneedle-based drug delivery systems: microfabrication, drug delivery, and safety. *Drug Deliv* 2010;17:187-207
87. Prausnitz MR, Langer R. Transdermal drug delivery. *Nat Biotechnol* 2008;26:1261-8
88. Prausnitz MR, Miskzta JA, Cormier M, et al. Microneedle-based vaccines. *Curr Top Microbiol Immunol* 2009;333:369-93
89. Henry S, McAllister DV, Allen MG, et al. Microfabricated microneedles: a novel approach to transdermal drug delivery. *J Pharm Sci* 1998;87:922-5
- **First proof of concept about microneedle study.**
90. Banks SL, Pinninti RR, Gill HS, et al. Flux across [corrected] microneedle-treated skin is increased by increasing charge of naltrexone and naltrexol in vitro. *Pharm Res* 2008;25:1677-85
91. Verbaan FJ, Bal SM, van den Berg DJ, et al. Improved piercing of microneedle

- arrays in dermatomed human skin by an impact insertion method. *J Control Release* 2008;128:80-8
92. Ding Z, Verbaan FJ, Bivas-Benita M, et al. Microneedle arrays for the transcutaneous immunization of diphtheria and influenza in BALB/c mice. *J Control Release* 2009;136:71-8
 93. Ding Z, Van Riet E, Romeijn S, et al. Immune modulation by adjuvants combined with diphtheria toxoid administered topically in BALB/c mice after microneedle array pretreatment. *Pharm Res* 2009;26:1635-43
 94. Mikszta JA, Alarcon JB, Brittingham JM, et al. Improved genetic immunization via micromechanical disruption of skin-barrier function and targeted epidermal delivery. *Nat Med* 2002;8:415-19
 95. McAllister DV, Wang PM, Davis SP, et al. Microfabricated needles for transdermal delivery of macromolecules and nanoparticles: fabrication methods and transport studies. *Proc Natl Acad Sci USA* 2003;100:13755-60
 96. Van Damme P, Oosterhuis-Kafeja F, Van der Wielen M, et al. Safety and efficacy of a novel microneedle device for dose sparing intradermal influenza vaccination in healthy adults. *Vaccine* 2009;27:454-9
 - **Clinical study against infection disease using microneedle device.**
 97. Matriano JA, Cormier M, Johnson J, et al. Macroflux microprojection array patch technology: a new and efficient approach for intracutaneous immunization. *Pharm Res* 2002;19:63-70
 98. Gill HS, Prausnitz MR. Coated microneedles for transdermal delivery. *J Control Release* 2007;117:227-37
 99. Zhu Q, Zarnitsyn VG, Ye L, et al. Immunization by vaccine-coated microneedle arrays protects against lethal influenza virus challenge. *Proc Natl Acad Sci USA* 2009;106:7968-73
 100. Chen X, Prow TW, Crichton ML, et al. Dry-coated microprojection array patches for targeted delivery of immunotherapeutics to the skin. *J Control Release* 2009;139:212-20
 101. Gill HS, Prausnitz MR. Coating formulations for microneedles. *Pharm Res* 2007;24:1369-80
 102. Kim YC, Quan FS, Compans RW, et al. Formulation and coating of microneedles with inactivated influenza virus to improve vaccine stability and immunogenicity. *J Control Release* 2010;142:187-95
 103. Kim YC, Quan FS, Compans RW, et al. Stability kinetics of influenza vaccine coated onto microneedles during drying and storage. *Pharm Res* 2011;28:135-44
 104. Hooper JW, Golden JW, Ferro AM, et al. Smallpox DNA vaccine delivered by novel skin electroporation device protects mice against intranasal poxvirus challenge. *Vaccine* 2007;25:1814-23
 105. Miyano T, Tobinaga Y, Kanno T, et al. Sugar micro needles as transdermic drug delivery system. *Biomed Microdevices* 2005;7:185-8
 106. Ito Y, Hagiwara E, Saeki A, et al. Feasibility of microneedles for percutaneous absorption of insulin. *Eur J Pharm Sci* 2006;29:82-8
 107. Ito Y, Yoshimitsu J, Shiroyama K, et al. Self-dissolving microneedles for the percutaneous absorption of EPO in mice. *J Drug Target* 2006;14:255-61
 108. Sullivan SP, Koutsonanos DG, Del Pilar Martin M, et al. Dissolving polymer microneedle patches for influenza vaccination. *Nat Med* 2010;16:915-20
 109. Matsuo K, Yokota Y, Zhai Y, et al. A low-invasive and effective transcutaneous immunization system using a novel dissolving microneedle array for soluble and particulate antigens. *J Control Release* 2012;161:10-17
 110. Matsuo K, Hirobe S, Yokota Y, et al. Transcutaneous immunization using a dissolving microneedle array protects against tetanus, diphtheria, malaria, and influenza. *J Control Release* 2012;160:495-501
 - **Efficacy against various antigens of dissolving microneedles.**
 111. Glenn GM, Rao M, Matyas GR, et al. Skin immunization made possible by cholera toxin. *Nature* 1998;391:851
 112. Tierney R, Beignon AS, Rappuoli R, et al. Transcutaneous immunization with tetanus toxoid and mutants of *Escherichia coli* heat-labile enterotoxin as adjuvants elicits strong protective antibody responses. *J Infect Dis* 2003;188:753-8
 113. Beignon AS, Briand JP, Muller S, et al. Immunization onto bare skin with synthetic peptides: immunomodulation with a CpG-containing oligodeoxynucleotide and effective priming of influenza virus-specific CD4+ T cells. *Immunology* 2002;105:204-12
 114. Ozaki T, Yauchi M, Xin KQ, et al. Cross-reactive protection against influenza A virus by a topically applied DNA vaccine encoding M gene with adjuvant. *Viral Immunol* 2005;18:373-80
 115. Kahlon R, Hu Y, Orteu CH, et al. Optimization of epicutaneous immunization for the induction of CTL. *Vaccine* 2003;21:2890-9
 116. Anjuere F, George-Chandy A, Audant F, et al. Transcutaneous immunization with cholera toxin B subunit adjuvant suppresses IgE antibody responses via selective induction of Th1 immune responses. *J Immunol* 2003;170:1586-92
 117. Medzhitov R, Preston-Hurlburt P, Janeway CA Jr. A human homologue of the *Drosophila* Toll protein signals activation of adaptive immunity. *Nature* 1997;388:394-7
 118. Manning BM, Enioutina EY, Visic DM, et al. CpG DNA functions as an effective adjuvant for the induction of immune responses in aged mice. *Exp Gerontol* 2001;37:107-26
 119. Seya T, Akazawa T, Tsujita T, et al. Role of Toll-like receptors in adjuvant-augmented immune therapies. *Evid Based Complement Alternat Med* 2006;3:31-8.discussion 133-137
 120. Thissen MR, Kuijpers DI, Krekels GA. Local immune modulator (imiquimod 5% cream) as adjuvant treatment after incomplete Mohs micrographic surgery for large, mixed type basal cell carcinoma: a report of 3 cases. *J Drugs Dermatol* 2006;5:461-4
 121. Johnston D, Bystryn JC. Topical imiquimod is a potent adjuvant to a weakly-immunogenic protein prototype vaccine. *Vaccine* 2006;24:1958-65
 122. Zhu J, Lai K, Brownile R, et al. Porcine TLR8 and TLR7 are both activated by a selective TLR7 ligand, imiquimod. *Mol Immunol* 2008;45:3238-43
 123. Combadiere B, Liard C. Transcutaneous and intradermal vaccination. *Hum Vaccin* 2011;7:811-27
 124. Kim YC, Park JH, Prausnitz MR. Microneedles for drug and vaccine delivery. *Adv Drug Deliv Rev* 2012;64:1547-68

S. Hirobe et al.

125. van der Maaden K, Jiskoot W, Bouwstra J. Microneedle technologies for (trans)dermal drug and vaccine delivery. *J Control Release* 2012;161:645-55
126. Celli S, Albert ML, Bousso P. Visualizing the innate and adaptive immune responses underlying allograft rejection by two-photon microscopy. *Nat Med* 2011;17:744-9
127. Ouchi T, Kubo A, Yokouchi M, et al. Langerhans cell antigen capture through tight junctions confers preemptive immunity in experimental staphylococcal scalded skin syndrome. *J Exp Med* 2011;208:2607-13

Affiliation

Sachiko Hirobe¹, Naoki Okada^{†2} PhD & Shinsaku Nakagawa^{*3} PhD

^{†*}Authors for correspondence

¹Assistant Professor,
Osaka University,
Graduate School of Pharmaceutical Sciences,
Laboratory of Biotechnology and Therapeutics,
1-6 Yamadaoka, Suita, Osaka 565-0871, Japan

²Associate Professor,
Osaka University,
Graduate School of Pharmaceutical Sciences,
Laboratory of Biotechnology and Therapeutics,
1-6 Yamadaoka, Suita, Osaka 565-0871, Japan
Tel: +81 6 6879 8176;
Fax: +81 6 6879 8176;
E-mail: okada@phs.osaka-u.ac.jp

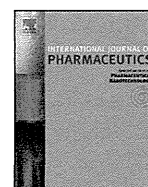
³Professor,
Osaka University,
Graduate School of Pharmaceutical Sciences,
Laboratory of Biotechnology and Therapeutics,
1-6 Yamadaoka, Suita, Osaka 565-0871, Japan
Tel: +81 6 6879 8175;
Fax: +81 6 6879 8179;
E-mail: nakagawa@phs.osaka-u.ac.jp



ELSEVIER

Contents lists available at SciVerse ScienceDirect

International Journal of Pharmaceutics

journal homepage: www.elsevier.com/locate/ijpharm

Performance and characteristics evaluation of a sodium hyaluronate-based microneedle patch for a transcutaneous drug delivery system

Yasuhiro Hiraishi^a, Takeshi Nakagawa^a, Ying-Shu Quan^b, Fumio Kamiyama^b, Sachiko Hirobe^a, Naoki Okada^{a,**}, Shinsaku Nakagawa^{a,*}

^a Laboratory of Biotechnology and Therapeutics, Graduate School of Pharmaceutical Sciences, Osaka University, 1-6 Yamadaoka, Suita, Osaka 565-0871, Japan

^b CosMED Pharmaceutical Co. Ltd., 32 Higashikujokawanishi-cho, Minami-ku, Kyoto 601-8014, Japan

ARTICLE INFO

Article history:

Received 29 August 2012

Received in revised form 9 October 2012

Accepted 30 October 2012

Available online 5 November 2012

Keywords:

MicroHyal[®]

Microneedle patch

Transcutaneous drug delivery

All-trans retinoic acid

ABSTRACT

The MicroHyal[®] microneedle (MN) patch was developed to provide a simple, safe, and effective drug delivery system. In this study, we examined the performance and characteristics of our fabricated MN patch to identify potential quality issues with future commercial application. Mechanical failure force analysis identified that the strength of the MN patch was affected by environmental humidity, because higher moisture levels weakened the strength of the MN. Incorporation of all-trans retinoic acid (ATRA) or ovalbumin (OVA) into the MN patch decreased the mechanical failure force by almost 50% of the strength of placebo (without drug) patches. ATRA-loaded MN patches displayed good stability after storage at 4 °C, with more than 90% and 85% of the drug remaining in the patch after 8 and 24 weeks of storage, respectively. Tetanus toxoid- and diphtheria toxoid-loaded MN patches stored for 12 months induced robust antigen-specific immune responses similar to the responses by freshly prepared MN patches. Fluorescence imaging findings suggested that prolonged antigen deposition was induced by MN-mediated fluorescein isothiocyanate-labeled (FITC)-OVA vaccination. Overall, although the strength of MN requires improvement, our developed MN patch appears to be an effective pharmaceutical product providing a simple, safe, and relatively painless approach.

© 2012 Elsevier B.V. All rights reserved.

1. Introduction

Transdermal drug delivery is an attractive administration option for small-molecule and macromolecule products, including vaccines, because of its accessibility, safety, painless drug administration, potential for self-administration, and avoidance of enzymatic degradation in the gastrointestinal tract or liver. However, the physical barrier of the stratum corneum, the outer layer of the skin, causes poor permeability across the skin and limits the bioavailability of macromolecules, thus limiting the progress of transdermal administration (Arora et al., 2008; Prausnitz, 2004; Prausnitz and Langer, 2008). To overcome this limitation, microneedle (MN) patches consisting of micron-scale needles

assembled on a transdermal patch have been developed using fabrication technology of the microelectronics industry (Kim et al., 2012a; Prausnitz et al., 2009).

Although MN technology was first developed in the early 1970s, few studies demonstrated its usefulness as a tool for transdermal drug delivery, until the advancement of microelectronics technology in the 1990s. MN fabrication technology has rapidly progressed since then. MNs have been made from silicon, metal, or polymer (Kim et al., 2012a; Kis et al., 2012). The majority of research papers published thus far used nondissolving MNs. Metal-based MNs coated with water-soluble formulations facilitate the successful delivery of agents such as insulin (Gill and Prausnitz, 2007), salmon calcitonin (Tas et al., 2012), parathyroid hormone (PTH; 1–34) (Ameri et al., 2010), hepatitis B surface antigen (Andrianov et al., 2009), inactivated influenza virus (Zhu et al., 2009), influenza virus-like particle (Quan et al., 2010), bacillus Calmette–Guérin (Hiraishi et al., 2011), and influenza virus hemagglutinin–DNA (Kim et al., 2012b; Song et al., 2012) into the skin.

Polymer MNs that dissolve in the skin have also been developed recently; these MNs display successful delivery and efficacy (Sullivan et al., 2010). Compared with metal-based MNs, polymer-based dissolving MNs have several potential advantages. Because polymer-based MNs dissolve completely in the skin, they cannot be

Abbreviations: MN, microneedle; ATRA, all-trans retinoic acid; TT, tetanus toxoid; DT, diphtheria toxoid; OV, ovalbumin; FITC–OVA, fluorescein isothiocyanate-labeled ovalbumin; HPLC, high-performance liquid chromatography; ERH, equilibrium relative humidity; ID, intradermal; PBS, phosphate-buffered saline; HSD, honestly significant difference; ANOVA, analysis of variance.

* Corresponding author. Tel.: +81 6 6879 8175; fax: +81 6 6879 8179.

** Corresponding author. Tel.: +81 6 6879 8176; fax: +81 6 6879 8176.

E-mail addresses: okada@phs.osaka-u.ac.jp (N. Okada), nakagawa@phs.osaka-u.ac.jp (S. Nakagawa).

intentionally reused, which may help prevent the transmission of blood-borne pathogens and diseases caused by reuse of needle and syringes in developing countries. In addition, they can completely eliminate biohazardous sharp waste after use and safety concerns such as fractured metal needles piercing the skin (Al-Zahrani et al., 2012).

In our earlier studies, we developed a sodium hyaluronate-based dissolving MN patch called MicroHyal[®]. Sodium hyaluronate is a component of skin tissue and is hydrophilic in nature; thus, it may be biocompatible with the skin and safe for exogenous material insertion, which has been verified by our recent study involving healthy human volunteers (submitted for publication). We also demonstrated that transcutaneous immunization using the MN patch induces immune responses against ovalbumin (OVA), adenoviral vectors, tetanus, diphtheria, malaria, and influenza, with comparable efficacy to traditional hypodermic needle-based immunization (Matsuo et al., 2012a,b). These safety and efficacy findings indicate that our developed MN patch is a promising delivery system. Considering its future commercial application, there are several critical attributes necessary for product quality. First, MNs need to be precisely inserted into the skin without mechanical failure in order to ensure drug delivery into the skin, which requires sufficient MN strength (Lee et al., 2008). Second, MNs should dissolve in the skin's interstitial fluid within no more than a few hours (hopefully within a few minutes) to minimize the patch application time; a shorter application time may be better from the point of view of patient compliance. Third, the stability of the drug loaded into the MN patch is an important factor for efficacy. Furthermore, thermostable vaccine formulations could facilitate increased vaccine coverage, especially in developing countries that lack an adequate healthcare infrastructure for cold-chain storage (Bell et al., 2001; Berhane et al., 2000).

In the present study, we investigated the performance and characteristics of a sodium hyaluronate-based MN patch. We evaluated the mechanical failure force of MNs and the dissolution characteristics of drugs from MNs. In addition, the stability performance of drug-loaded MN patches was assessed using all-trans retinoic acid (ATRA; vitamin A acid) and the tetanus toxoid (TT)/diphtheria toxoid (DT) divalent vaccine as model compounds. We also described the deposition of antigen in mouse skin by *in vivo* fluorescence imaging after MN administration using comparisons with traditional hypodermic needle-based intradermal (ID) administration.

2. Materials and methods

2.1. Animals

Six-week-old female Wistar-ST rats and 7- to 10-week-old female ICR mice were purchased from Japan SLC Inc. (Hamamatsu, Japan). Seven- to nine-week-old female HR-1 hairless mice were purchased from SHIMIZU Laboratory Supplies Co., Ltd. (Kyoto, Japan). All animals were housed at the Osaka University animal facility. All animal studies were conducted in accordance with the guidelines provided by the Animal Care and Use Committee of Osaka University.

2.2. Fabrication of the dissolving MN patch

As described previously (Matsuo et al., 2012b), the dissolving MN patch was fabricated at CosMED Pharmaceutical Co. Ltd., (Kyoto, Japan) using micromolding technologies with sodium hyaluronate as the base material. Previously developed MN contained collagen. In this study, we used a collagen-free MH as collagen is suspected to induce inflammation in human. In brief,

sodium hyaluronate (JP grade, Kikoman Biochemifa Company, Tokyo, Japan), dextran 70 (JP grade, Meito Sangyo, Nagoya, Aichi), and Polyvidone (JPE grade, BASF Japan, Tokyo, Japan) were dissolved in distilled water at a ratio of 11:8:1 and then mixed with ATRA (Sigma-Aldrich Inc., St. Louis, MO, USA), OVA (Sigma-Aldrich Inc.), fluorescein isothiocyanate-labeled-OVA (FITC-OVA; Molecular Probes, Eugene, OR, USA), or the TT/DT divalent vaccine (The Research Foundation for Microbial Diseases of Osaka University, Suita, Japan). The aqueous solution was casted onto micromolds and then dried in a desiccator at room temperature. The dissolving MN patches were obtained by removing them from the micromolds. Placebo dissolving MN patches were also fabricated in the same manner, without an active pharmaceutical ingredient. The MN patches contained more than 200 MNs/cm². To form the MN transcutaneous patch system, patches with an area of 0.8 cm² were fixed onto an adhesive film with a surface area of 2.3 cm². Hence, our dissolving MN patch system consisted of the MicroHyal[®] patch with MNs that were 200 (MH200), 300 (MH300), or 800 μ m (MH800) in length.

2.3. Moisture conditioning and moisture content measurement of the MN patch

To condition the MN patch to different moisture contents, the patch was placed in desiccators containing Tri-Sorb molecular sieves (Süd-Chemie Performance Packaging, Colton, CA, USA) or a saturated solution of potassium acetate (Wako Pure Chemical, Osaka, Japan), magnesium chloride hexahydrate (Wako Pure Chemical), potassium carbonate (Wako Pure Chemical), or sodium chloride (Wako Pure Chemical). The desiccators were stored at room temperature (25 °C) for 1 week in an environment of 0, 22, 33, 44, or 75% relative humidity (RH) (Young, 1967). After removal of the MN patch from the desiccator, the endpoint moisture level was evaluated as a function of equilibrium relative humidity (ERH) using a water activity analyzer (HygroLab; Rotronic AG, Bassersdorf, Switzerland).

2.4. Measurement of mechanical failure force for MNs

The force necessary for mechanical MN fracture was measured using a TA-XT plus texture analyzer (StableMicro Systems, Surrey, UK). An MN patch was attached to a test station by double-sided adhesive tape. Axial force was then applied using a flathead 5-mm diameter stainless steel cylinder to move the cylinder at a rate of 0.6 and 1.1 mm/min for MH300 and MH800, respectively, and the trigger force was set at 0.049 N.

2.5. Quantification of ATRA loaded into the MN patch

To determine the amount of ATRA loaded into the MN patches, MNs were first removed from the base material using a razor. The removed MNs were soaked in distilled water followed by vortex mixing to completely dissolve them. Ethanol (Wako Pure Chemical) was added to the sample solution followed by vortex mixing, and the sample solution was then diluted with acetonitrile (Wako Pure Chemical). The sample solution was filtered through a membrane filter (0.45- μ m diameter) and analyzed using a high-performance liquid chromatography (HPLC) method, as reported previously (Tashtoush et al., 2007). In brief, a D-2000 Elite HPLC system (Hitachi, Tokyo, Japan) was used. Chromatographic separation was performed using a reverse-phase Nucleosil 5 μ m C18 100A column (250 mm \times 4.6 mm; GL Science Inc., Tokyo, Japan). The mobile phase comprised 0.01% trifluoroacetic acid and acetonitrile (15:85, v/v) at a flow rate of 1 ml/min. The column temperature was 40 °C, and the detection wavelength was 342 nm. The concentration of ATRA in the sample solution was determined using a standard curve

based on known concentrations of ATRA, which was converted to the absolute mass of ATRA loaded into the MN patch with a dilution factor. The ATRA MN patch was packaged in a heat-sealed aluminum laminated sachet under a refrigerated condition (4 °C) or at room temperature (25 °C) to examine the shelf-life.

2.6. Dissolution of ATRA from MNs and delivery to skin

MNs were imaged by brightfield stereomicroscopy (VHX-1000; Keyence Corporation, Osaka, Japan). To prevent moisture uptake by environmental humidity that may affect needle failure force and dissolution characteristics, MN patches were packed in moisture impermeable package, heat-sealed aluminum laminated sachet, before use, and used for the study immediately after opening the package. The back skin of the HR-1 hairless mice was pierced with the ATRA-loaded MN patch (MH800) using a handheld applicator (Matsuo et al., 2012b) under isoflurane inhalation anesthesia. The patch was left in place for 30, 60, or 120 min and covered with a wound management film (BIOCLUSIVE; Johnson & Johnson Medical, Ltd., Tokyo, Japan). After removing the patch, the efficiency of drug delivery into the skin was determined by comparing (i) the residual amount of ATRA on the MN patch after skin insertion, (ii) the amount of ATRA deposited onto the skin surface, and (iii) the amount initially loaded. The amount of ATRA deposited onto the skin surface was evaluated by applying adhesive tape (Scotch tape, 3M, St. Paul, MN, USA) to the skin surface; immersing the tape in distilled water, ethanol, and acetonitrile (6:4:90, v/v); and determining the amount of ATRA by HPLC. Using a mass balance, the amount of ATRA delivered into the skin was determined by subtracting the amount remaining on the MN patch and on the skin surface after insertion from the amount originally on the noninserted MN patch.

2.7. Fluorescence imaging for antigen deposition assessment

Hair on the back of the ICR mice was shaved using clippers and completely removed using a depilatory lotion (Kracie, Tokyo, Japan) under isoflurane inhalation anesthesia. This hair removal protocol is frequently employed in our laboratory for MN vaccination studies and is similar to procedures used in the literature (Hiraishi et al., 2011). The FITC-OVA (1 µg protein)-loaded MN patch was administered. The patch was pressed into the skin using a handheld applicator and left in place for 60 min covered with a wound management film. After removal of the patch, the skin was harvested, frozen in OCT compound (Sakura Finetechnical Co., Ltd., Tokyo, Japan), and cut into 8-µm-thick sections using a cryostat. Histological examination of the skin was performed on frozen sections that were mounted with Prolong Gold antifade reagent with DAPI (Invitrogen, Carlsbad, CA) and then photographed using fluorescence microscopy (BZ-8000; Keyence Corporation, Osaka, Japan).

To perform *in vivo* fluorescence imaging, the HR-1 hairless mice were treated with an FITC-OVA (10 µg protein)-loaded MN patch (MH300), ID injection of phosphate-buffered saline (PBS) containing FITC-OVA (10 µg protein/30 µl), or ID injection of FITC-OVA (10 µg protein/30 µl) that was removed from the MN patch and reconstituted by ID injection in PBS on the back skin under isoflurane inhalation anesthesia. The reconstituted solution consisted of 10 µg FITC-OVA, 386 µg sodium hyaluronate, 284 µg dextran 70, and 36 µg polyvidone in 30 µl PBS. Fluorescence images were obtained using the CRi Maestro EX *in vivo* imaging system (Cambridge Research and Instrumentation, Woburn, MA). To capture the FITC image, a blue filter for excitation at 455 nm and a blue emission filter at 515 nm were used. The exposure time was 200 ms, and spectral resolution for all imaging was 10 nm. Measurements of

integrated fluorescence intensity for the injection site were made by Maestro version 2.10 software.

2.8. Vaccination and ELISA assay for IgG

To evaluate the stability of the hyaluronate-based MN patch, combined TT (20 µg) and DT (10 µg)-loaded MN patches (MH800) were stored at 4, 25, or 40 °C for up to 12 months before vaccination. Hair on the back of the Wistar-ST rats was removed using clippers and a depilatory lotion. The stored MN patch was pressed into the skin using a handheld applicator under isoflurane anesthesia, covered with a wound management film, and left in place for 6 h. The freshly prepared MN patches were also administered as a comparable vaccination. Vaccinations were repeated 5 times every 2 weeks. At the indicated periods, sera were collected from the rats to determine the antigen-specific IgG titers by ELISA according to previously described protocols (Matsuo et al., 2011). The endpoint titers of antigen-specific antibodies were expressed as the reciprocal log₂ of the last dilution that had an absorbance value of 0.1 absorbance units after subtracting the background.

2.9. Challenge study for tetanus toxin

For the challenge study, the rats vaccinated with stored MN patches were subcutaneously injected in the hind leg with a lethal dose (1 µg) of tetanus toxin (Sigma-Aldrich, Inc.) 1 month after the final vaccination. The rats were observed daily for 4 days to record mortality.

2.10. Statistical analysis

The data obtained were analyzed by Student's *t*-test, Tukey-Kramer's honestly significant difference (HSD) test, or analysis of variance (ANOVA) using JMP software ver. 8.0 (SAS Institute Inc., Cary, NC, USA). In all cases, *p* < 0.05 was considered significant.

3. Results

3.1. Fabrication of the MN patch and investigation of mechanical failure force

MN patches fabricated using micromolding technologies were designed to be sufficiently long to penetrate across the stratum corneum barrier and into the skin but sufficiently short to prevent pain (Gill et al., 2008). The MNs used in this study were 200 (MH200), 300 (MH300), or 800 µm (MH800) in length.

To assure drug delivery into the skin, MNs need to be precisely inserted into the skin without mechanical failure. The mechanical failure force of MNs was assessed according to a previously described method (Park et al., 2005). A force displacement curve revealed that force initially increased with the displacement of the stainless steel cylinder pressed against MNs, followed by a sudden decline in force, which was interpreted as the point of MN failure (Fig. 1A). After the failure force test, MNs were evaluated by brightfield stereoscopic microscopy (Fig. 1B).

Because of the hygroscopic nature of sodium hyaluronate, our fabricated MN patch may easily absorb moisture after exposure to high humidity, which may affect needle strength. We first conditioned MN patches to various humidity conditions, obtaining MN patches with different moisture levels. The moisture level of the MN patch was assessed as the water activity of ERH (Heidemann and Jarosz, 1991). After 1 week of storage in a desiccator, the moisture levels changed relative to the storage humidity (Fig. 2A). The water activity of the MN patch before storage was 18.5%, and this increased to 59.1% after storage at 75% RH for 1 week. We next

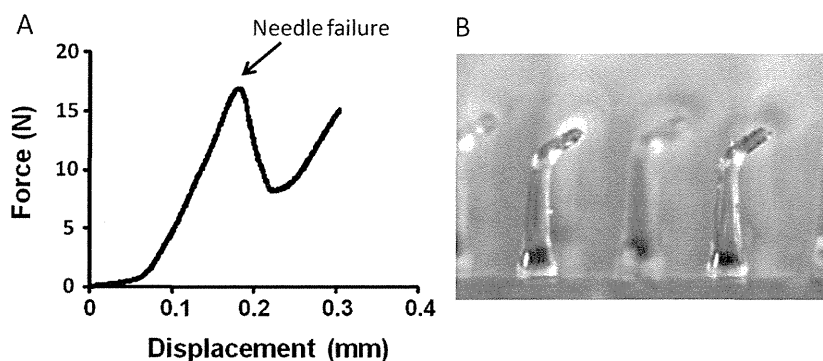


Fig. 1. Mechanical failure force analysis of microneedles (MNs). Force was measured as a function of the displacement of the stainless steel cylinder pressed against the MNs. (A) Representative failure behavior of MNs under an axial load. Needle failure was identified by a sudden drop in force. (B) Brightfield stereomicrograph of MNs after an axial failure test.

measured the mechanical failure force of MNs using the moisture-conditioned MN patches (Fig. 2B). Data are presented as the force per needle required for failure using a needle density and the flat surface area of the stainless steel cylinder for axial loading. The mechanical failure force was dependent on the moisture level of the MN patch (ANOVA, $p < 0.01$). When the water activity of the patch was 59.1%, the failure force was 0.14 N per needle, which

was nearly 50% lower than that of a dried MN patch (18.5% water activity after storage at 0% RH).

To better understand the influence of active pharmaceutical ingredients on needle strength, ATRA and OVA were selected as our model small molecule and macromolecule compounds, respectively, and loaded into MN patches. The failure forces of ATRA MNs were less than 0.1 N per needle, with ranges of 0.04–0.056 N for MH300 (Fig. 3A) and 0.073–0.1 N for MH800 (Fig. 3B). Compared with the failure force of placebo MNs (Fig. 2B), the failure force was decreased by approximately 50% on incorporation of ATRA. The amount of ATRA in the MN patch did not affect the failure force at the amounts evaluated (ANOVA, $p > 0.05$). Similarly, the failure forces of OVA MNs (Fig. 3C, D) were lower than those of placebo MNs, irrespective of the amount of OVA loaded (ANOVA, $p > 0.05$).

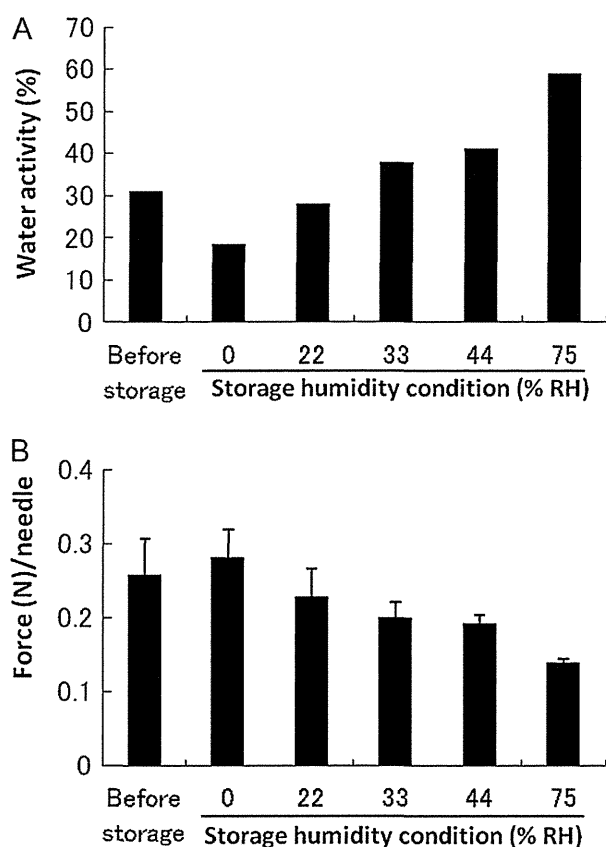


Fig. 2. Water activity and mechanical failure force for placebo MNs. (A) Water activity of MH800 after storage under various humidity conditions. The water activity was measured using a water activity analyzer. As a control, the water activity before storage was also measured. (B) Mechanical failure force of MH800 as a function of water activity. The force required to fracture 55 MNs was measured using a TA-XT plus texture analyzer. Data represent the average \pm standard deviation of 3 measurements each.

3.2. Dissolution characteristics of MNs

In our previously published studies, we demonstrated that placebo MNs completely dissolved in 60 min after insertion into mouse or rat skin (Matsuo et al., 2012b). In this study, we selected ATRA as a model compound to evaluate the dissolution characteristics of drug-loaded MNs. Because of the poor water solubility of ATRA (Didja et al., 1989), we considered it a good model compound for evaluating the dissolution capability of our fabricated MNs for comparisons with placebo or water-soluble compound-loaded MNs.

Brightfield micrographs of ATRA MNs before and after insertion demonstrated that the MNs were almost completely dissolved 120 min after application (Fig. 4A). To better understand the degree of ATRA delivery, the amount of ATRA delivered into the skin was measured using HPLC by subtracting the amount of drug remaining in the MN patch and on the skin surface after insertion from the amount originally loaded into the noninserted MN patch. After insertion into the skin for 120 min, almost all the ATRA was released into the skin at a delivery rate exceeding 90% (Fig. 4B). However, 60 min of application was not sufficient for complete delivery (76% delivery rate), and the needle bottom remained on the base material (Fig. 4A).

3.3. Localization and deposition of antigen delivered by the MN patch

To monitor the delivery of antigen into the skin, the mice were administered FITC-OVA as a model antigen. Fig. 5 represents histological sections of the insertion site in mouse skin after insertion of the MNs for various application times. The resulting needle track crossed the epidermis and into the superficial dermis and revealed that antigen was delivered (green spot) to both of these layers. With

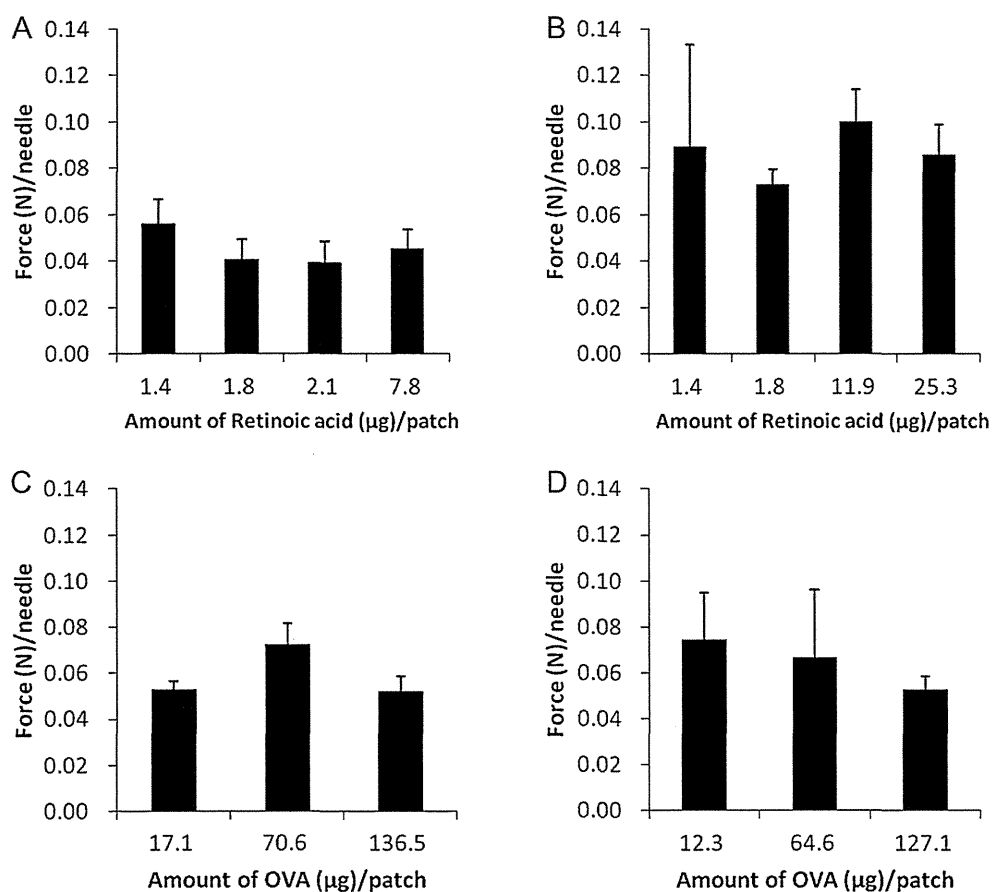


Fig. 3. Mechanical failure force for MNs as a function of the amount of drug loaded. (A) All-trans retinoic acid (ATRA)-loaded MH300, (B) ATRA-loaded MH800, (C) ovalbumin (OVA)-loaded MH300, and (D) OVA-loaded MH800. Data represent the average \pm standard deviation of 3 measurements each.

a 3-h application time, antigen remained around the insertion site. With longer application times, the antigen gradually diffused in the superficial dermis.

We next monitored the deposition of antigen *in vivo* after administration of FITC-OVA into mouse skin using the FITC-OVA-loaded MN patch by drawing comparisons between ID immunization using an FITC-OVA PBS solution or reconstituted FITC-OVA solution obtained from the MN patch using a 26-gauge hypodermic needle. Fluorescence micrographs demonstrated that the amount of antigen injected by the ID method reduced drastically 3 h after administration, whereas a slight green spot remained up to 47 and 24 h when the reconstituted solution and PBS solution were injected intradermally, respectively (Fig. 6A). In contrast, intense antigen deposition corresponding to the administration site of the MN patch was observed up to 47 h after administration, and a small green spot remained after 74 h. Fig. 6B shows the kinetics of the integrated fluorescence intensity for the injection site, which indicated that MN patch administration resulted in prolonged antigen deposition compared with other administration methods.

3.4. Stability performance of the MN patch

ATRA is known to be chemically unstable. When ATRA is exposed to light, heat, or oxidants, it is rapidly degraded into isomerized products (Brisaert et al., 1995; Lim et al., 2004). To evaluate the stability performance of our sodium hyaluronate-based MN patch and its possible shelf-life, we selected ATRA as a model compound. ATRA MN patches packaged in heat-sealed aluminum

laminated sachets were stored in a refrigerated condition (4 °C) for 3 different manufacturing lots or at room temperature (25 °C) for 1 lot. The amount of ATRA in the MN patch was assayed by HPLC and expressed as the percentage of the initial (without storage) amount (Fig. 7). The amount of ATRA in the patch was significantly reduced after storage at room temperature (25 °C) for 1 week ($78.1 \pm 11.6\%$, Student's *t*-test, $p < 0.05$), and continued storage up to 24 weeks resulted in additional loss of ATRA to $44.8 \pm 23.3\%$ (Student's *t*-test, $p < 0.05$). Conversely, there was no significant loss of ATRA under the refrigerated condition (4 °C) for 24 weeks ($86.1 \pm 5.4\%$, Student's *t*-test, $p = 0.08$), and all 3 lots exhibited similar trends for stability during refrigerated storage.

We next used the combined TT/DT-loaded patches in an additional stability assessment. The vaccination efficacies of antigen-specific IgG titers were evaluated as a stability characteristic indicator. The vaccination protocol and animal model (rat) were those of previously reported methods (Matsuo et al., 2012a). The TT/DT-loaded MN patches were exposed to various storage conditions and then administered into the exposed back skin of rats. After 6 months of storage at 4, 25, or 40 °C in heat-sealed aluminum laminated sachets, both anti-TT and anti-DT IgG titers increased with increasing numbers of vaccinations (Fig. 8A, B). Continued storage for up to 12 months at the same temperatures (Fig. 8C, D) followed by vaccination also resulted in the induction of pronounced antigen-specific IgG levels comparable with those induced by freshly prepared MN patches (Tukey–Kramer HSD, $p > 0.05$). Furthermore, the storage temperature did not affect the immune response induced by loaded TT (20 µg) and DT (10 µg) (ANOVA,

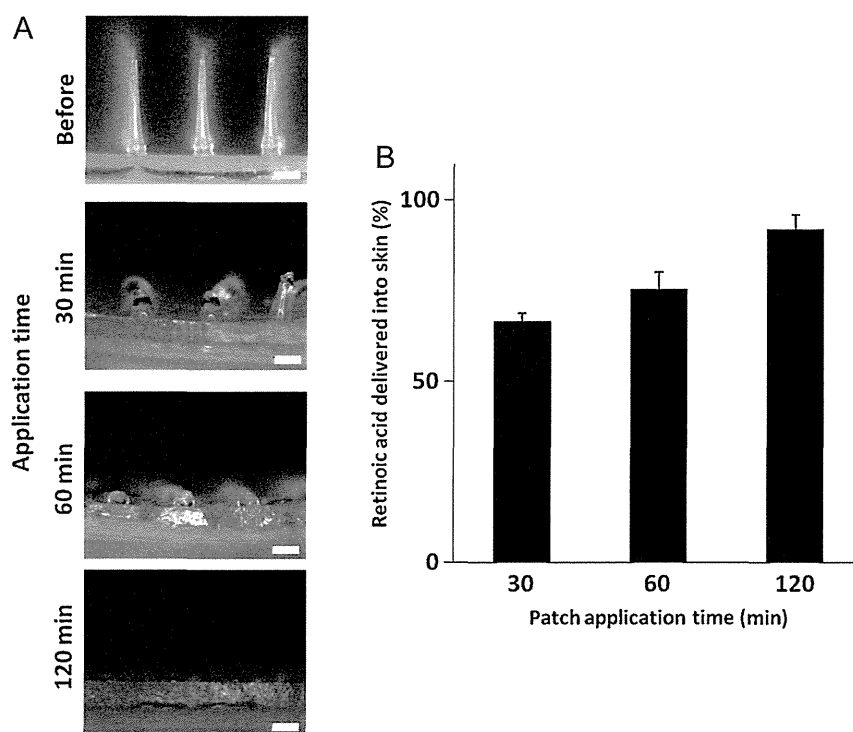


Fig. 4. Dissolution of ATRA-loaded MNs. (A) Stereoscopic micrographs of MNs (scale bar, 200 μm). The MN patches were pressed into the back skin of HR-1 hairless mice and left for 30, 60, or 120 min. After 120 min, almost all the MNs were dissolved. (B) Percentage of ATRA delivered into the skin as a function of the application time.

$p > 0.05$). Although further investigation is necessary with lower antigen amounts and different animal species, these results support that our MN patch was highly immunogenic in rats even after long-term storage for 12 months.

To ensure the immunogenicity of the stored MN patch, we conducted a challenge study. The rats vaccinated with the stored MN patches were injected with a lethal dose of 1 μg tetanus toxin 1 month after the final vaccination. The nonvaccination group was not included in this study because of animal care guidelines. The rats were observed daily for 4 days to record mortality. The data illustrated that all animals vaccinated using the stored MN patches survived the tetanus toxin challenge (Table 1).

4. Discussion

Over the past 15 years, the field of MN technology has rapidly progressed, with more than 350 research papers being published. Many pharmaceutical companies have entered this field. The Soluvia[®] microinjection system consisting of short, hollow, steel needles is now available for vaccination (Kim et al., 2012a). The metal-based MN patch from ZOSANO has moved into a Phase II clinical trial for the administration of PTH (1–34) for treating osteoporosis (Cosman et al., 2010). With regard to dissolving polymer MN patches, to our knowledge, no commercially available products are yet available in the pharmaceutical field. Our MicroHyal[®] patch is the only dissolving MN patch available; it has only been used for cosmetic products. For further exploration of our patch in the pharmaceutical field, we have been investigating the possibility of its application in vaccination. We have demonstrated its effectiveness with various antigens (Matsuo et al., 2012a,b). As a next step, we are investigating the possibility of commercial application. Commercial products require several attributes to assure their quality, such as dissolution of a drug from the MN patch and identification of the degradation products. Assays of content uniformity, needle strength, aseptic integrity, and stability

performance will be required for the MN patch. In this study, as an initial step to assess these attributes, we evaluated the needle strength, dissolution characteristics, and stability of the patch using model compounds. Furthermore, the therapeutic use of ATRA as a dermatological treatment (Darlenski et al., 2010), antitumor agent (Ozpolat and Lopez-Berestein, 2002; Zuccari et al., 2005), and immunomodulator (Skountzou et al., 2006) motivated us to evaluate the feasibility of ATRA MN patches.

Our MicroHyal[®] patch is composed of sodium hyaluronate as a base material. Sodium hyaluronate may be biocompatible as it is a skin tissue component that is hydrophilic in nature. This will be advantageous for safety. However, its hydrophilic nature may adversely affect needle strength when the MN patch is exposed to environmental humidity, and this could be a critical issue for usage and storage in high humidity environments, especially in *WHO Climatic Zone IV* countries (Kopp, 2006). The mechanical failure force test results indicated that the needle strength decreased as the moisture level of the MN patch increased. To simulate its usage in high humidity conditions, MN patches (MH800) were stored at 55% RH and 25 $^{\circ}\text{C}$ or 95% RH and 37 $^{\circ}\text{C}$ for 30 min. Then, the patches were pressed into the back skin of ICR mice using the handheld applicator. After removal of the MN patch, the MNs remaining on the patch were examined. The MNs stored at 55% RH and 25 $^{\circ}\text{C}$ were successfully pressed on the skin of the mice, and they dissolved into the skin. In contrast, the MNs stored at 95% RH and 37 $^{\circ}\text{C}$ bent from the needle bottom, and they could not be pressed into the skin (Supplementary Fig. S1). These data suggested that the MN patch should be packaged in a moisture-impermeable container before use, and immediate use after opening a package is recommended. Facilitating increased vaccination coverage, especially in developing countries lacking adequate healthcare infrastructures, requires further improvement in the strength of the needle to improve its stability in high humidity by optimizing the base components. For optimization of base material, we plan to perform a material screening using a moisture sorption isotherm for a material,

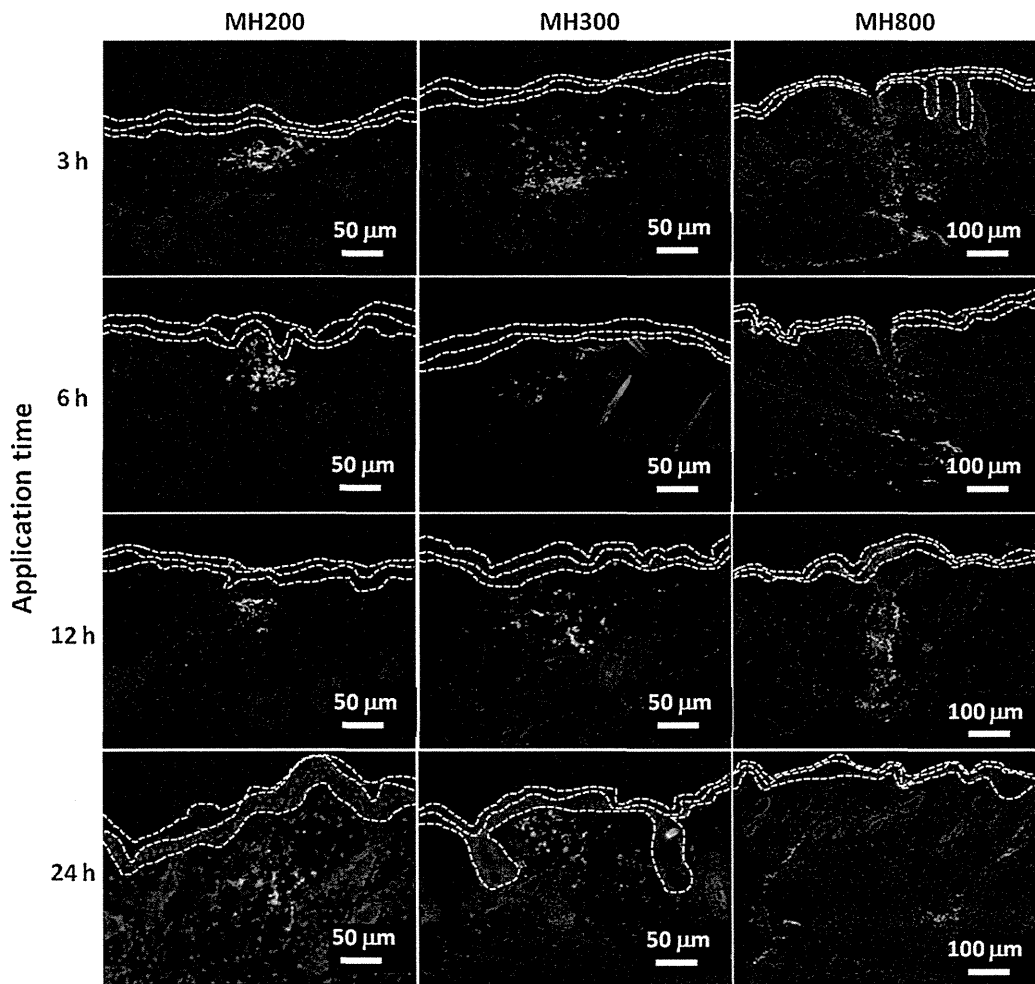


Fig. 5. Histological section of the back skin of ICR mice treated with fluorescein isothiocyanate-labeled (FITC)–OVA-loaded MH200, MH300, or MH800 for 3, 6, 12, or 24 h. After removal of the MN patch, the skin was harvested and frozen. Frozen sections (8- μm -thick) were photographed using a fluorescence microscope. The resulting needle track crossed the epidermis and into the superficial dermis, revealing that FITC–OVA was delivered (green spot) to both these layers. The nucleus was counterstained using DAPI (blue). The white dotted lines indicate the surfaces of the stratum corneum, epidermis, and superficial dermis, respectively, from top to bottom.

which is the relationship between water content and equilibrium humidity of a material. Preferable material for dissolving MNs need to show low moisture content at the environmental humidity of 11–75%RH to keep sufficient needle strength, and high moisture content at high humidity of more than 90%RH to dissolve quickly. We currently consider adding a disaccharide as an improvement option.

We also found that incorporating ATRA or OVA decreases the needle strength compared with the strength of placebo MNs (no

active pharmaceutical ingredient). According to a previous report, the insertion force required for MNs with a tip diameter of 25 μm to pierce the skin is 0.058 N per needle (Park et al., 2005). Our fabricated MN has a tip diameter of 30 μm , which may require a similar insertion force as that reported by Park et al. For a sufficient safety margin for skin insertion by application of gentle force by the thumb, the needle strength must exceed 0.058 N per needle. However, the needle strength of ATRA- or OVA-loaded MNs was less than 0.1 N per needle (Fig. 3). In this study, there was

Table 1
Rat tetanus toxin challenge study.

Vaccination ^a			Tetanus toxin (μg) ^b	Survival ratio (survival rat/tested rat)
Storage condition	Method	TT (μg)		
4 °C for 6 months	MNs	20	1	5/5
25 °C for 6 months	MNs	20	1	5/5
40 °C for 6 months	MNs	20	1	5/5
4 °C for 12 months	MNs	20	1	5/5
25 °C for 12 months	MNs	20	1	5/5
40 °C for 12 months	MNs	20	1	5/5

^a Vaccinations were repeated 5 times every 2 weeks.

^b Tetanus toxin (1 μg) was subcutaneously injected in the hind leg.